THE STATIC AND DYNAMIC CHARACTERISTICS OF SERIES-CONNECTED TUNNEL DIODES AND THEIR APPLICATIONS IN DIGITAL CIRCUITS

by

CLEMENT ANDRE TEWFIK SALAMA

B.A.Sc., University of British Columbia, 1961

A THESIS SUBMITTED IN PARTIAL FULFILMENT OF

THE REQUIREMENTS FOR THE DEGREE OF

MASTER OF APPLIED SCIENCE

in the Department

of

Electrical Engineering

We accept this thesis as conforming to the

required standard

THE UNIVERSITY OF BRITISH COLUMBIA

December, 1962

In presenting this thesis in partial fulfilment of the requirements for an advanced degree at the University of British Columbia, I agree that the Library shall make it freely available for reference and study. I further agree that permission for extensive copying of this thesis for scholarly purposes may be granted by the Head of my Department or by his representatives. It is understood that copying or publication of this thesis for financial gain shall not be allowed without my written permission.

Department of Electrical Engineering

The University of British Columbia,
Vancouver 8, Canada.

Date January 10th, 1963

ABSTRACT

A multistable composite volt-ampere characteristic can be realized using a number of tunnel diodes. A maximum of 2^n stable states can be obtained using n suitably chosen tunnel diodes connected in series. The main purpose of this study is to investigate the static and dynamic characteristics of such a circuit.

Preliminary work deals with the switching behaviour of a single tunnel diode and the dependence of the switching time on the figure of merit and the current overdrive. This work serves as a background to the study of the multistate circuit.

The study of the static characteristics of the composite device determines the conditions necessary for the generation of the required number of stable states. Additional conditions necessary to ensure proper operation are derived from the study of dynamic characteristics of a two tunnel diode multistate circuit. The dynamic conditions derived involve the tunnel diode capacitances and their ratio. The temperature dependence of the circuit is also investigated. Experimental results are presented showing an operating speed of 12.5 ns for a four state circuit using available tunnel diodes.

The versatility of the composite characteristic obtained, and the inherent high speed of the tunnel diodes combine to make the multistate device useful in high-speed digital applications such as: binary addition, analog-to-digital conversion, and counting. These applications are discussed briefly.

ACKNOWLEDGEMENT

The author is indebted to Dr. M.P. Beddoes, the supervising professor of this project, for his help and guidance throughout the course of this research.

Grateful acknowledgement is given to the Northern Electric Company Limited for a Fellowship awarded in 1961, and to the National Research Council for a Studentship awarded in 1962.

The work described in this thesis was supported by the National Research Council under Grant (BT-68).

TABLE OF CONTENTS

LIST OF ILLUSTRATIONS

LIST OF TABLES

LIST OF SPECIAL SYMBOLS AND TERMS

Symbol		First Defined in Section
V_P =	Diode Peak Voltage	2.1
V_V =	Diode Valley Voltage	2.1
V_F =	Diode Forward Voltage	2.1
I_P =	Diode Peak Current	2.1
I_V =	Diode Valley Current	2.1
m_r^* =	Reduced Electron mass (relative) in a Semiconductor Material	2.1
E_g =	Energy Gap in a Semiconductor Material .	2.1
ϵ_r =	Relative Dielectric Constant	2.1
Z =	Tunneling Probability	2.1
$f(v)$ =	Diode v-i Characteristic	2.3
$C(v)$ =	Diode Capacitance	2.3
C_V =	Diode Valley Capacitance	2.3
$\|r\|$ =	Magnitude of the Diode Negative Resistance	3.
C/I_P =	Figure of merit	3.
$C\|r\|$ =	Figure of merit	3.
T_2 =	Precursor Pulse Duration	4.6
δI_V =	Difference in the Valley Currents of the Two Diodes	4.8

Term	
Percent Overdrive:	3.2
Rise Time:	3.2
Delay Time:	3.2
Switching Time:	3.2
Precursor Pulse:	4.6

THE STATIC AND DYNAMIC CHARACTERISTICS OF SERIES-CONNECTED TUNNEL DIODES AND THEIR APPLICATIONS IN DIGITAL CIRCUITS

1. INTRODUCTION

A great variety of negative resistance devices have been made from semiconductor materials; a recent one is the tunnel diode.[1]

In the past several years, widespread interest has been shown in the use of tunnel diodes in digital circuits. The reason for this interest lies in the tunnel diode's inherent advantages: high switching speed, low power dissipation, device simplicity, small size, and high stability with changes in environmental conditions such as temperature and nuclear radiation. There are, however, difficulties in obtaining gain and directionality using the device.

The advent of the tunnel diode revived the interest in the use of the volt-ampere characteristics of several interconnected negative resistance devices to generate multistable composite characteristics. The form and the complexity of the composite characteristics depend on the individual devices and the mode of connection. The complex characteristics generated can lead to a host of ways of using negative resistance devices in the performance of digital logic functions. One interesting combination of n negative resistance devices connected in series was found to generate 2^n stable states,[2] provided the individual devices obey certain rules.

The main purpose of the following study is to investigate

the static and dynamic characteristics of such a combination using tunnel diodes as negative resistance elements.

The thesis consists of four main sections. The first introductory section deals with the tunnel diode as a negative resistance element. The operation of the device, its volt-ampere characteristic, and its equivalent circuit are discussed briefly.

The second section deals with the behaviour of a single tunnel diode and its possibilities and limitations as a switching device. The analysis is carried out by computer solution of the circuit equations. Experimental results are used to verify these solutions. The investigation in this section provides a necessary background to the discussion in the next two sections.

The third section deals with the static and dynamic characteristics of the series-connected tunnel diode circuit. First, a graphical analysis of the composite characteristic, supported by experimental results, establishes the relationship that the static parameters of the individual tunnel diodes must satisfy in order to generate the required multistable composite characteristic. Next, the dynamic behaviour of a tunnel diode multistate circuit is investigated by a computer simulation of the non-linear system, and verified by experiment. This investigation establishes some additional relations complementing the conditions derived from the static analysis to ensure proper operation.

The fourth and last section deals with possible applications of the multistate composite devices in the performance of digital functions such as binary addition, analog-to-digital conversion, and counting.

2. THE TUNNEL DIODE AS A NEGATIVE RESISTANCE DEVICE

The tunnel diode is essentially a narrow p-n junction, made of very highly doped semiconductor material, which exhibits a negative resistance over a limited (several tenths of a volt) voltage range when biased in the forward direction. The negative resistance is of the non-parametric[3] type and arises from the so called "tunneling" mechanism, a strictly quantum mechanical effect.

In a normal rectifying p-n diode, conduction in the forward direction occurs predominantly by the diffusion of minority carriers across the p-n junction: these carriers consist of holes which diffuse from the p - side to the n - side, and electrons which travel in the opposite direction. Both contributions, because of the difference in the sign of the charge, constitute a conventional current of the same sign.

However, in a narrow p-n junction (of the order of 150 Angstroms) which is heavily doped with controlled impurities, the Fermi level E_F, instead of falling within the forbidden gap, as for the rectifying diode, falls within the valence band on the p - side and within the conduction band on the n - side as shown in Figure 2-1. This causes an overlap Δ of the band edges, and it gives rise to a new conduction mechanism: the so called "tunnel effect" or internal field emission first considered by Zener[4]. Electrons in a given energy state in the valence band can, without changing their energy state, "tunnel" through the forbidden gap into the empty or conduction band and vice versa under the action of a large electric field.

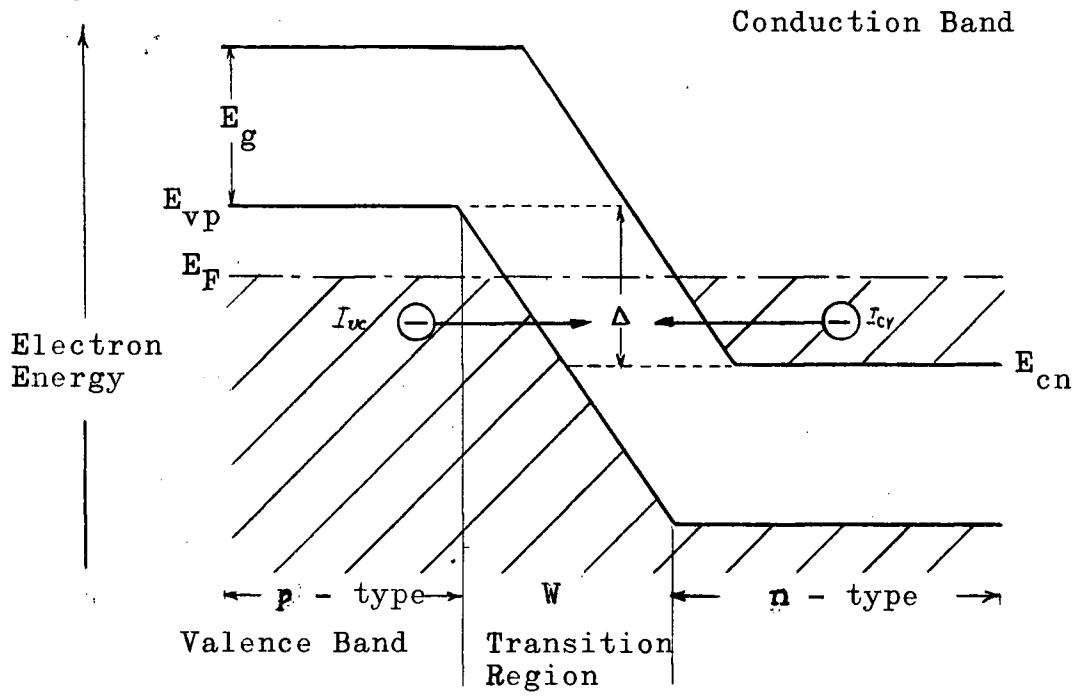

Figure 2-1. Energy-band Scheme at Junction of a Tunnel Diode at Thermal Equilibrium.

As mentioned above, the only electrons involved in the tunneling process are those falling in states included in the band overlap Δ. Since charges of one sign are involved, the two components of current (due to oppositely moving charges) must be subtracted from each other. In particular, with no external bias applied, the net current must be zero; therefore exact cancellation must take place, though each component by itself is non-zero. On the other hand, the net current vanishes for a forward voltage which just destroys the overlap, but in this case the individual components are also zero. For

intermediate voltages, a net forward current flows because the rates of change of these two components with bias voltage differ. Thus for increasing bias voltage, the current increases, reaches a peak, and then decreases producing a negative incremental resistance.

2.1 Volt-Ampere Characteristic of a Tunnel Diode.

The low frequency characteristic of a typical tunnel diode is shown in Figure 2-2 together with the important d-c parameters. It differs from that of any other type of p-n junction in that it exhibits a "hump" of current giving rise to the negative resistance. Tunnel diodes have been made with peak currents ranging from 10 microamperes to 10 amperes. However, for a given semiconductor material, the voltage scale must remain fixed to a large extent, and it is determined by the energy gap of the semiconductor. Hence, the tunnel diode is a low voltage device, the power range of which can be extended only by increasing its current.

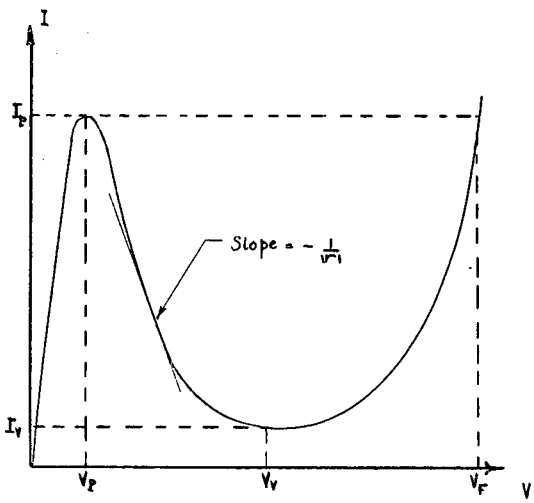

V_P = Peak Voltage
V_V = Valley Voltage
I_P = Peak Current
I_V = Valley Current
V_F = Forward Voltage at I_P

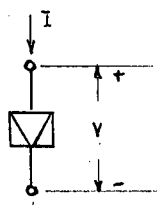

Figure 2-2. D-C Characteristic of a Tunnel Diode.

Tunnel diodes have been made from a number of semiconductor materials. Table 2.1 lists five of them together with some of their properties.[5],[6],[7]

Type of Semiconductor	Properties of Semiconductor Materials			Properties of Tunnel Diodes (Typical Values)	
	E_g(ev.)	m_r^*	ε_r	I_P/I_V	V_F(v)
GaAs	1.35	0.13	11.1	40	1
Si	1.11	0.78	11.2	4	0.7
Ge	0.67	0.44	16	15	0.48
InAs	0.33	0.051	11.7	12	0.25
InSb	0.18	0.028	15.9	10	0.14

m_r^* = reduced electron mass (relative)

E_g = energy gap

ε_r = relative dielectric constant

Table 2.1 Properties of Tunnel Diodes and Semiconductor Materials Used in Their Fabrication

Tunneling, as a quantum mechanical process, has been treated in considerable detail in the literature,[1],[6],[7],[8],[9] and only a brief discussion will be given here to explain the details of the volt-ampere characteristic curve. At low forward voltage, a high current flows through the diode due to band-to-band tunneling; at sufficiently high voltage, current flows by forward injection. Between these two voltage ranges, the current is unexpectedly high and has been called the "excess" current.

First consider the tunneling current;[1] as stated previously, this current consists of two components flowing across the junction in opposite directions; I_{vc} from the valence

to the conduction band, and I_{cv} flowing from the conduction band to the valence band. The current I_{cv} at any energy level E is proportional to the number of electrons in the conduction band, the number of available states in the valence band, and the tunneling probability from the conduction band to the valence band. Letting $\rho_c(E)$ and $\rho_v(E)$ represent the energy state densities in the conduction and valence bands respectively, $f_c(E)$ and $f_v(E)$ the corresponding Fermi distribution functions denoting the probability that a given energy state is occupied, and Z_{vc} and Z_{cv} the tunneling probabilities in the two directions. Then $f_c(E)\,\rho_c(E)$ = density of conduction-band electron states occupied in dE,

$(1 - f_v(E))\,\rho_v(E)$ = density of valence-band electron states unoccupied in dE.

Thus

$$I_{cv} = A \int_{E_{cn}}^{E_{vp}} Z_{cv}\ \rho_c(E)\ f_c(E)\ \left[1 - f_v(E)\right] \rho_v(E)\ dE \qquad \ldots(2\text{-}1)$$

where A is the junction area; and the interval of integration is from the conduction-band edge of the n - side E_{cn}, to the valence band edge of the p - side E_{vp}, i.e., through the band overlap (Figure 2-1).

Similarly

$$I_{vc} = A \int_{E_{cn}}^{E_{vp}} Z_{vc}\, \rho_v(E)\, f_v(E)\, \left[1 - f_c(E)\right] \rho_c(E)\, dE \qquad \ldots(2\text{-}2)$$

The general shape of the two tunneling components as well as the net tunneling current $(I_{cv} - I_{vc})$ are shown in Figure 2-3.

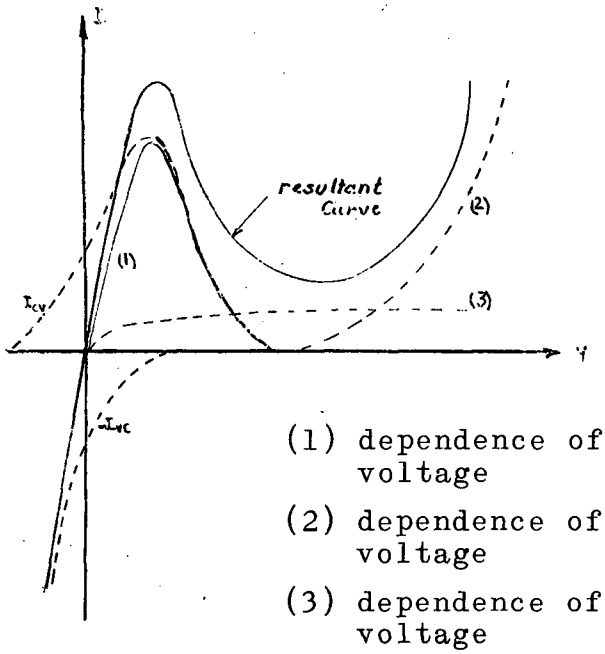

(1) dependence of the Tunnel Current on voltage

(2) dependence of the Diffusion Current on voltage

(3) dependence of the Excess Current on voltage

Figure 2-3. Components of the Volt-Ampere Characteristic of a Tunnel Diode.

Next consider the excess current which occurs at forward voltages in the range where the electrons in the degenerate donor levels in the n - side have been raised to energies greater than those of the degenerate acceptor levels in the p - side. Ideally, tunneling of electrons from the conduction

to the valence band, in a single energy-conserving transition, should then be impossible and only the diffusion current due to the forward injection of minority carriers should flow. In practice as Yajima and Esaki[6] first noted, the actual current at such biases is considerably in excess of the normal diffusion current: hence the term excess current. The excess current is primarily due to the tunneling process since its behaviour generally parallels that of the peak current; the peak and excess currents exhibit much of the same dependence on pressure, on temperature, and on the donor and acceptor concentrations that make up the junction.[11]

A few hypotheses have been proposed to explain the interband tunneling transitions in the excess current range; however, there is now a growing amount of evidence that the excess current is caused by electrons tunneling not completely through the energy gap, but only part of the way, making use of more or less localized imperfection energy levels present in the energy gap. This mechanism was first suggested by Esaki and, subsequently, several authors[11],[12] have obtained strong confirmation of it, by showing that the magnitude of the excess current can be altered by deliberately changing the imperfection content of the crystal, either by suitable doping or by radiation damage.

Based on a theoretical analysis of such a mechanism, curve (3) Figure 2-3 represents an approximation adopted by Kane[9] for the dependence of the excess current on the voltage applied to the tunnel diode.

2.2 Temperature Dependence of Tunnel Diode D-C Parameters.

The tunnel diode d-c parameters are temperature dependent. Figure 2-4 shows the variation of the d-c parameters with temperature for a T1925 Germanium tunnel diode. As shown the peak current decreases by 4% as the temperature is lowered from room temperature to -60°C. Slightly beyond room temperature, the peak current decreases with increasing temperature. The valley current, as shown, increases monotonically with temperature. This behaviour is expected because of the increase in energy gap and decrease in tunneling as the temperature is lowered, and because of the smearing out of the Fermi function at high temperatures.[13] The peak voltage V_P and forward voltage V_F decrease nearly linearly with increasing temperature at rates of about 0.06 mv/°C and 1.0 mv/°C respectively.

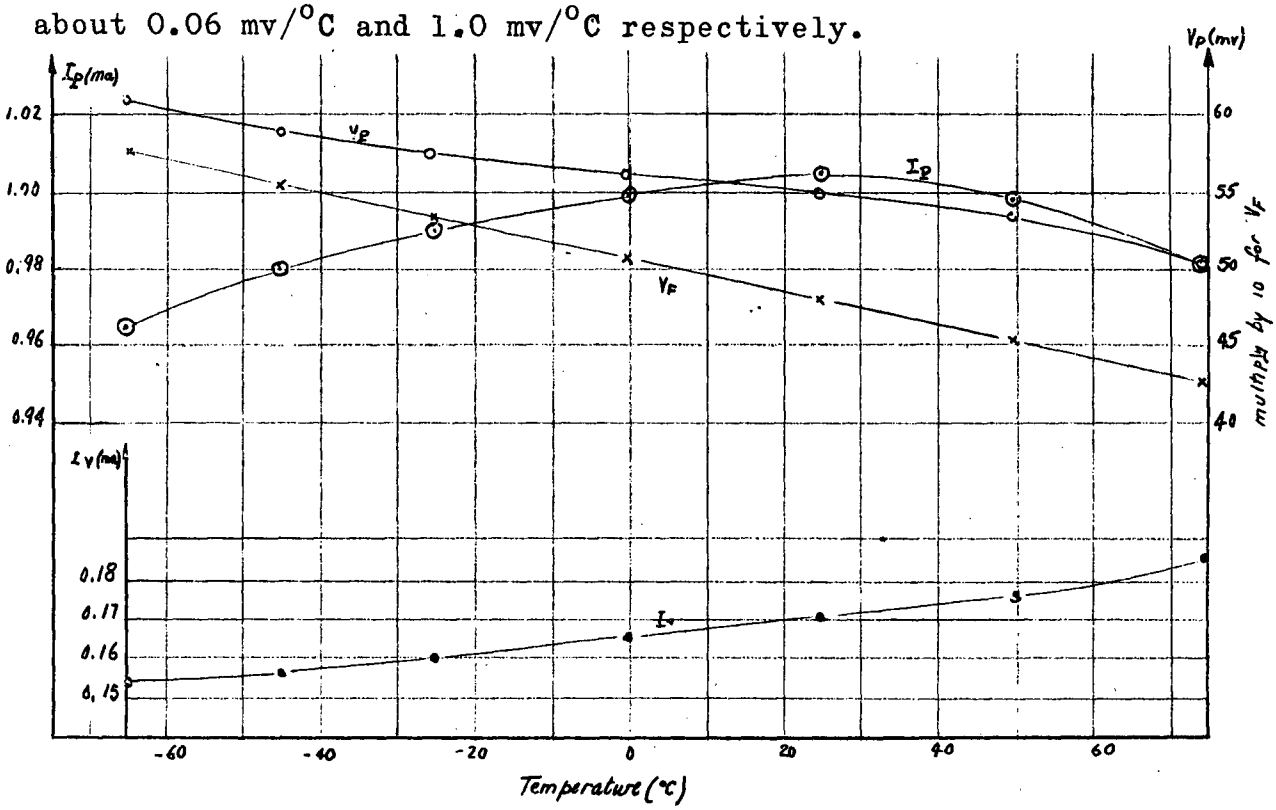

Figure 2-4. Variation of Tunnel Diode D-C Parameters with Temperature.

2.3 Tunnel Diode Equivalent Circuit.[7]

The tunnel diode is a voltage controlled negative resistance device (VCNR). For small signal applications, the tunnel diode is satisfactorily characterized by its differential negative resistance (-r), its junction capacitance C, series bulk resistance r_d and its housing inductance L_d, as shown in Figure 2-5(a). However, for large signal and switching mode applications, which are the main concern of this thesis, the equivalent circuit of Figure 2-5(a) was extended.[8] The large signal equivalent circuit, shown in Figure 2-5(b), consists of three elements in series: an inductance L_d, a resistance r_d and a voltage dependant capacitance C(v) shunted by a non-linear current generator f(v) representing the non-linear d-c characteristic of the tunnel diode. The tunneling phenomenon is very fast and no delay effects are included in the current generator; the junction capacitance is assumed to represent all the storage mechanism in this device.

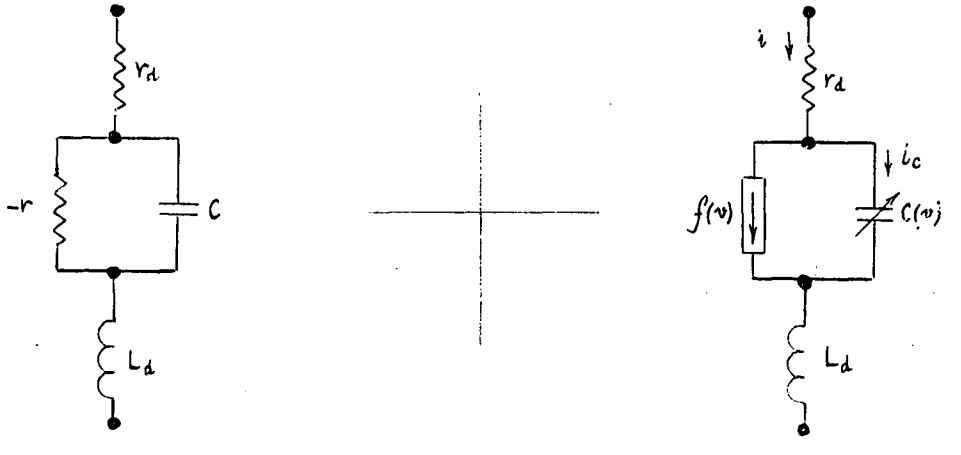

(a) Small Signal (b) Large Signal

Figure 2-5. Equivalent Circuits of Tunnel Diodes.

Measurements of the tunnel diode equivalent circuit parameters have been dealt with extensively in the literature; [14],[15],[16] and only a method aimed at measuring the capacitance variation with voltage is considered in Appendix I (experimental results are included). Theoretically, the variation of C with voltage may be approximated by:

$$C(v) = C_0 \left[1 - \frac{v}{V_g} \right]^{-n} \qquad n \simeq \tfrac{1}{2} \qquad \ldots(2\text{-}3)$$

where C_0 is the capacitance of the tunnel diode at zero voltage, and V_g is the voltage gap or the voltage for which the capacitance would theoretically go to infinity. The experimental results indicate that the exponent n varies between 0.4 and 0.5. It will be useful to define here the valley capacitance C_V as given by the following equation:

$$C_V(V_V) = C_0 \left[1 - \frac{V_V}{V_g} \right]^{-n} \qquad n \simeq \tfrac{1}{2} \qquad \ldots(2\text{-}4)$$

The most important parameter in the equivalent circuit, apart from the capacitance, is the non-linear current generator f(v) representing the v - i characteristic. The lack of a satisfactory theoretical[9],[17],[18] expression for f(v) led to the use of analytical approximations which are dealt with in Appendix II.

3. SINGLE TUNNEL DIODE SWITCHING BEHAVIOUR

As a first step, it was thought worthwhile to analyse the performance of a single tunnel diode and investigate its possibilities as a switching device. Against this background is developed the main subject of the thesis: a treatment of the static and dynamic behaviour of an interesting combination of series-connected tunnel diodes.

Starting with one tunnel diode, a digital computer simulation of the pertinent non-linear system was carried out. Experimental results were found to verify the general behaviour predicted by the computer solutions. The mathematical analysis clarifies diode operation and provides a useful rule of thumb for the switching time as a function of the device's figure of merit. The figure of merit[21],[22] of the diode is usually expressed as either the C/I_P or $C\,|r|$ constant of the diode; where C is the capacitance, $|r|$ is the magnitude of the average negative resistance and I_P is the peak current. Empirically, the relation between the $C\,|r|$ and C/I_P constants is given approximately by the following equation (for a Ge tunnel diode):

$$\left[C\,|r|\right](\text{sec.}) \cong 10^{10}\left[C/I_P\right](\text{pf/ma})$$

The figure of merit and its dependence on various parameters such as doping, energy gap etc., will be considered first; the subsequent analysis will be purely mathematical, without any physical consideration of the detailed mechanism of

tunneling. This mathematical approach may be entirely justified because the time constant of tunneling determined by the dielectric relaxation time[23] (10^{-13} sec.) is much smaller than the C |r| time constant (10^{-11} sec.). In other words the equivalent circuit of section 2.3 is valid over the wide frequency range of interest.

3.1 Dependence of the Figure of Merit on the Electrical Parameters of the Junction.

The tunneling current through a narrow p-n junction (Figure 2-1) in any semiconductor is proportional to the tunneling probability $\mathbf{Z} = \mathbf{Z}_{vc} = \mathbf{Z}_{cv}$ (see equation 2-1). The tunneling probability **Z** has been evaluated[9] for individual electron transitions across a region of constant field F, in terms of F, the energy gap E_g and the reduced mass of the electron m^* and is given by:

$$\mathbf{Z} = \exp\left[-\frac{\pi^2\, m^{*\frac{1}{2}}\, E_g^{3/2}}{e\, h\, F}\right] \qquad \ldots(3\text{-}1)$$

where

h = Planck's constant,

e = electronic charge.

Defining an average F by: We $F = E_g$, where the width W of an abrupt junction is given by:[24]

$$W = \left[\left(\frac{N + P}{NP}\right)\frac{2\,\varepsilon\, E_g}{e^2}\right]^{\frac{1}{2}}$$

ε being the dielectric constant, and N, P the doping levels on the n and p sides of the junction respectively. Substituting for F in equation 3-1 we get:

$$Z = \exp\left[-\frac{\sqrt{2}\,\pi^2}{eh}\,(m^*\,\varepsilon\,\frac{N+P}{NP})^{\frac{1}{2}}\,E_g\right] \qquad \ldots(3\text{-}2)$$

The junction capacitance C and the peak current I_P are given by:

$$C = \frac{\varepsilon A}{W}\,, \qquad \ldots(3\text{-}3)$$

$$I_P = A\,Z\int_E\,,$$

where $\int_E$ stands for the tunneling integral (eqs. 2-1, 2-2) and A is the junction area. Therefore:

$$C/I_P = \frac{\alpha\left[\frac{\varepsilon(NP)}{(N+P)\,E_g}\right]^{\frac{1}{2}}\exp\left[\beta(m^*\,\varepsilon\,\frac{N+P}{NP})^{\frac{1}{2}}\,E_g\right]}{\int_E} \qquad \ldots(3\text{-}4)$$

where α and β are constants.

For high levels of doping, the exponential factor becomes the dominant factor in the above expression. Thus for a given semiconductor the figure of merit is not a constant but depends on the doping concentration: the higher the concentration the lower the figure of merit and the faster the switching.

For a given doping concentration, the negative resistance (-r) is inversely proportional to the tunneling

probability Z and depends only to a small extent on the density of states. Thus equations 3-2 and 3-3 show that materials with small band gaps, small dielectric constants, and small effective masses have the smallest C | r | time constants.

For the purpose of comparison, referring back to Table 2.1 which lists the material constants of several semiconductors, we can see that InSb and InAs are the materials with the lowest figures of merit.

3.2 Tunnel Diode Switching Speed.

The diode represented by the equivalent circuit (Figure 3-1(a)) could be an amplifier, oscillator or switching element, according to the values of the d-c source voltage V_0, the external resistance R, and the inductance L. This inductance represents the total series inductance of the circuit including the tunnel diode lead inductance.

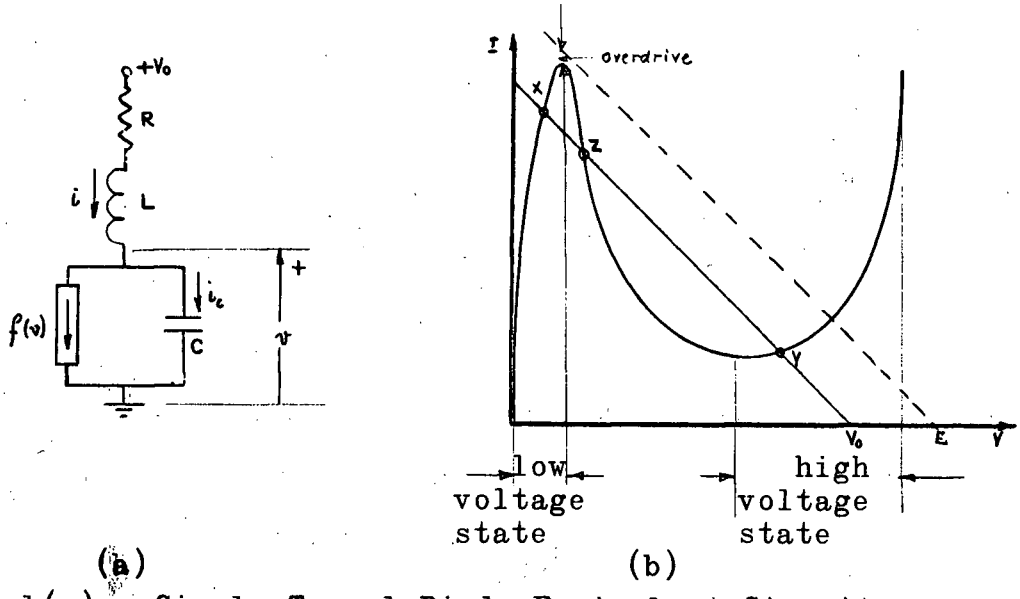

Figure 3-1(a). Single Tunnel Diode Equivalent Circuit

(b). Tunnel Diode Characteristic Illustrating Switching Load Line.

The stability criteria[16] of the circuit dictate that the negative resistance portion of the tunnel diode characteristic is an unstable region if the total circuit positive resistance is larger than the minimum magnitude of the negative resistance of the diode. Consequently the tunnel diode can only switch through this region provided $R \geq |r|_{min}$. Figure 3-1(b) shows the switching load line superimposed on the tunnel diode characteristic. The load line intersects the characteristic in three points, two of which (x,y) are stable and one is unstable (z).

Defining the current i, f(v) and i_c as shown in Figure 3-1(a); the equations describing the large signal behaviour of the tunnel diode circuit are:

$$C \frac{dv}{dt} = i - f(v) \qquad \ldots(3\text{-}5)$$

$$L \frac{di}{dt} = E - Ri - v \qquad \ldots(3\text{-}6)$$

$$i_c = i - f(v) \qquad \ldots(3\text{-}7)$$

where v = the terminal voltage of an ideal diode excluding the voltage drop across the diode's series resistance,

$E = V_0 + v_s$; $\quad V_0$ = d-c source voltage,

v_s = triggering source voltage,

$f(v)$ = a seventh order polynomial (given by equation AII-1) which closely fits the observed v-i characteristic of a 1 ma Ge tunnel diode (T1925),

C = tunnel diode capacitance assumed constant and equal to the valley capacitance.

It should be mentioned that equations 3-5, 3-6 are invariant to the following substitutions:

$$C' = aC \qquad L' = \frac{L}{a} \qquad R' = \frac{R}{a} \qquad i'_c = ai_c \qquad \text{and } i' = ai \qquad \ldots(3\text{-}8)$$

or $$C' = bC \qquad L' = bL \text{ and } t' = bt \qquad \ldots(3\text{-}9)$$

where a and b are numerical constants. Therefore we may deal with a diode for which $C = 10$ pf and $I_p = 1$ ma without loss of generality.

In the following analysis, the tunnel diode was biased in two different modes: a current mode $R_c = R >> |r|_{min}$ (horizontal load line), and a voltage mode $R_v = R > |r|_{min}$. The switching in both cases was investigated. However, before analyzing the results it will be useful to define the "overdrive" [26],[27] associated with a given input signal. The percent of overdrive is the excess in current at the diode peak voltage as a percent of the diode peak current.

Case I: Current Bias

The tunnel diode was biased by a constant d-c current source at approximately half the peak current I_p. Prior to

switching, the diode was in its low voltage state. Switching was accomplished by the application of a positive trigger current, defined here as a step-function current source in parallel with the d-c power supply.

When the diode is driven from a current source, the "small" series inductance of the tunnel diode is swamped by the source resistance and does not affect the dynamic behaviour of the overall circuit. In this case ($L=0$, $R=R_c$), the equations describing the network may be expressed in the simplified form:

$$C \frac{dv}{dt} = i - f(v) \qquad \ldots(3\text{-}10)$$

$$i_c = i - f(v)$$

where $i = I_0 + i_s$; I_0 = d-c bias current,

i_s = trigger current.

Equation 3-10 was solved by the Runge-Kutta-Gill[28] method using the IBM 1620 computer. Figure 3-2 shows the waveforms of the voltage across the diode for various overdrive factors.

The switching time is customarily defined as the time for either the voltage- or current-change to reach 90% of the total change expected. For the case under consideration only the voltage switching time is significant. A closer investigation of the switching transients in Figure 3-2 shows that the switching time can be divided into a "delay time", which is the time

required for a 0 to 10% change in output voltage; and a "rise time", which is the time required for a 10% to 90% change in output voltage. Figure 3-3 shows the variation of switching time, rise time and delay time with overdrive.

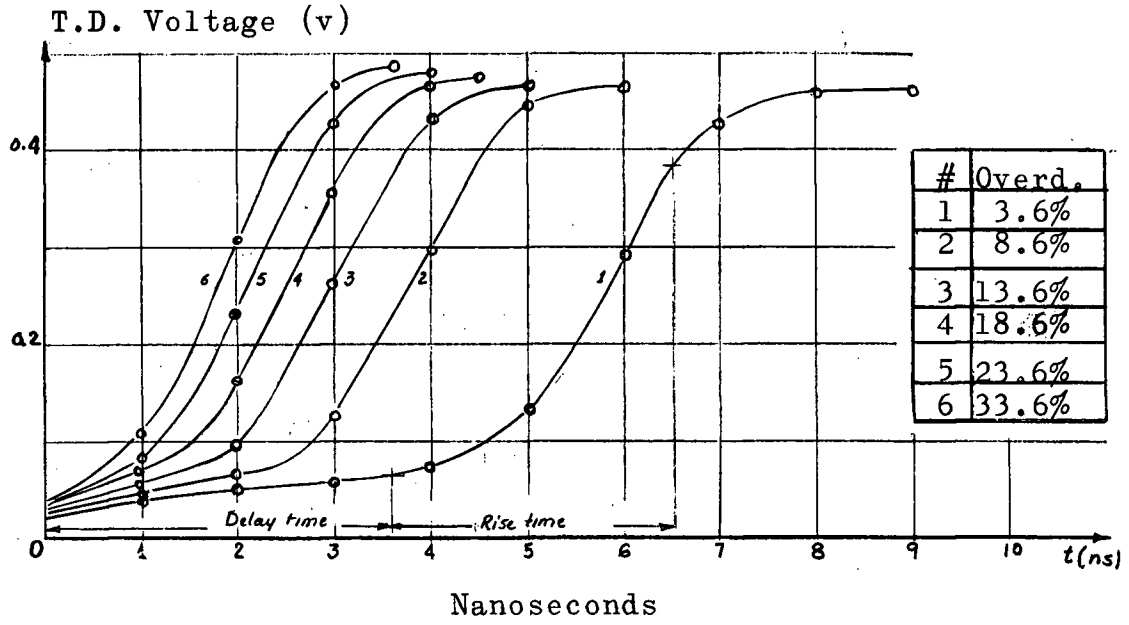

Nanoseconds

Figure 3-2. Switching Transient v(t) for Various Overdrive Factors. ($C = 10$ pf, $I_p = 1$ ma, $R = R_c$)

It is observed that the variations in overdrive have the apparent effect of changing the delay of the output waveform to a much greater extent than the rise time[22]. This is due to the fact that for small overdrive the capacitive current is small near the diode peak voltage, and this results in a slow rate of change of voltage in the initial stage of the transient.

To make the curves of Figure 3-3 more generally applicable, the switching and delay times were normalized with respect to the characteristic $C|r|$ time constant and plotted

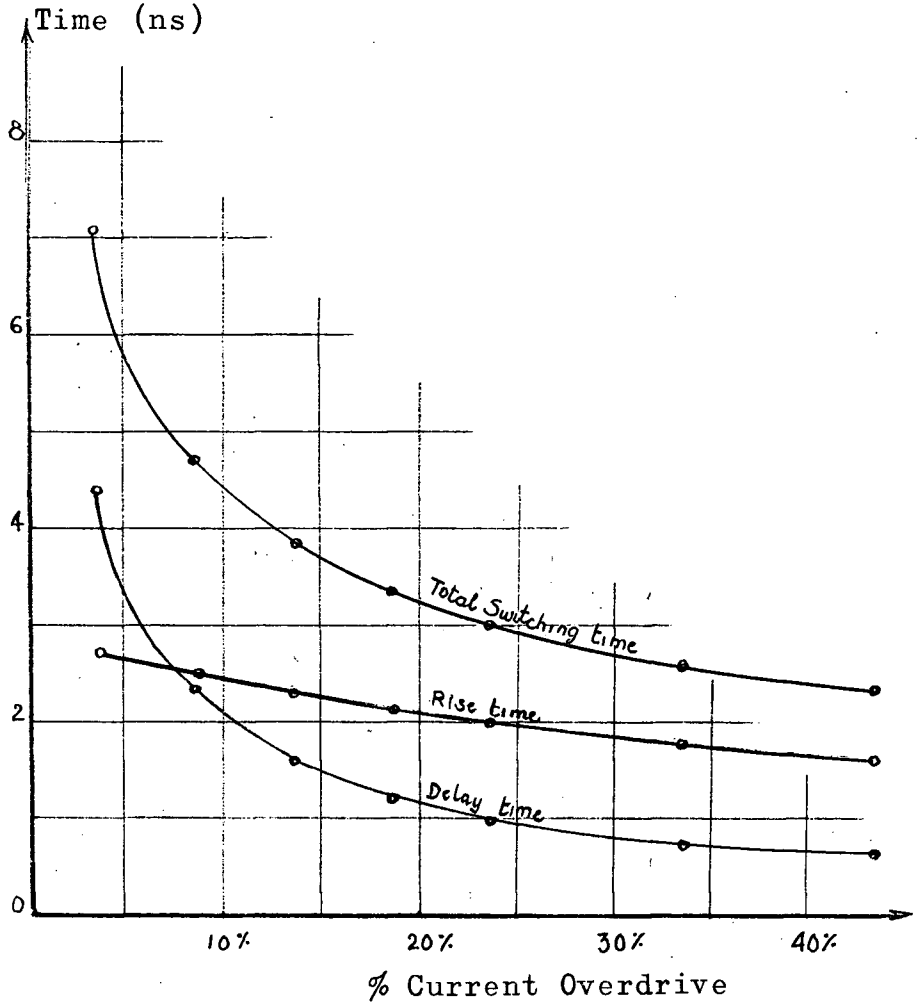

Figure 3-3. Switching Time, Delay Time and Rise Time versus Overdrive ($C = 10$ pf, $I_P = 1$ ma, $R = R_c$).

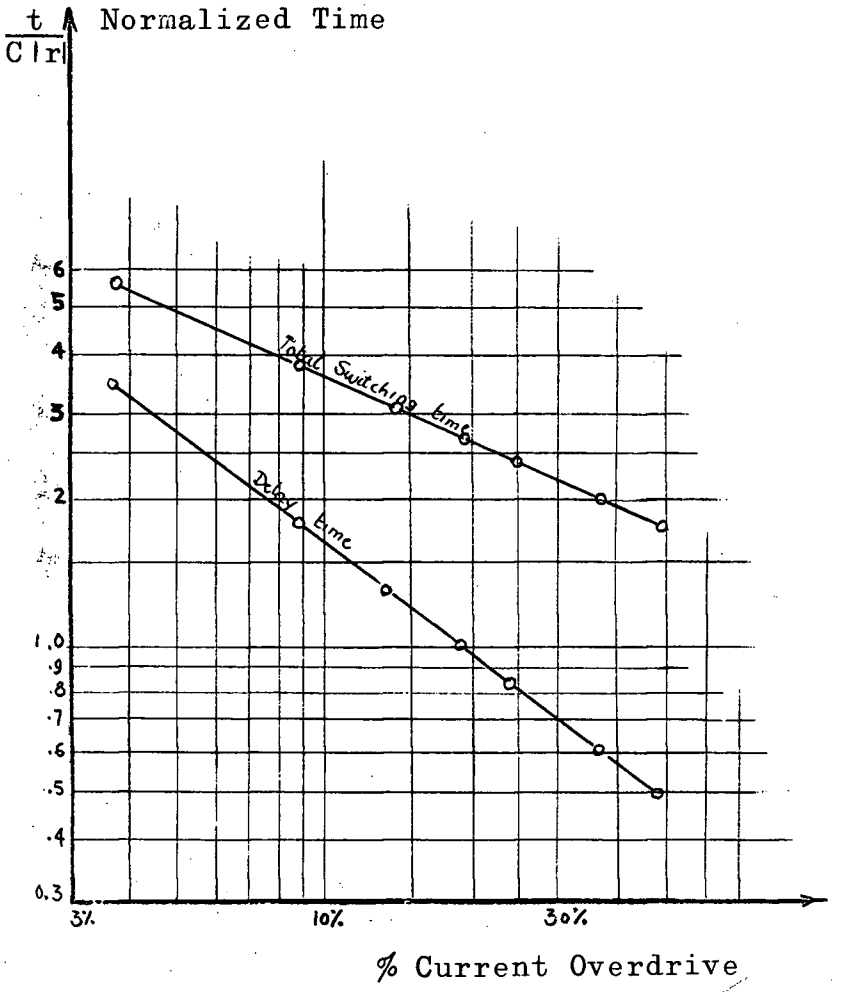

Figure 3-4. Normalized Switching and Delay Time versus Overdrive ($R = R_c$).

versus overdrive on a log-log scale in Figure 3-4. Given the C |r| time constant of a Ge diode, we can deduce from Figure 3-4, its switching and delay times for a given overdrive factor.

The importance of the delay time in the operation of tunnel diode switching circuits is evident. Figure 3-5 shows the delay time for 10% overdrive as a function of the diode capacitance and peak current. For example a 10 pf, 1 ma diode has a delay of 2 ns. (ns = nanosecond = 10^{-9} sec.)

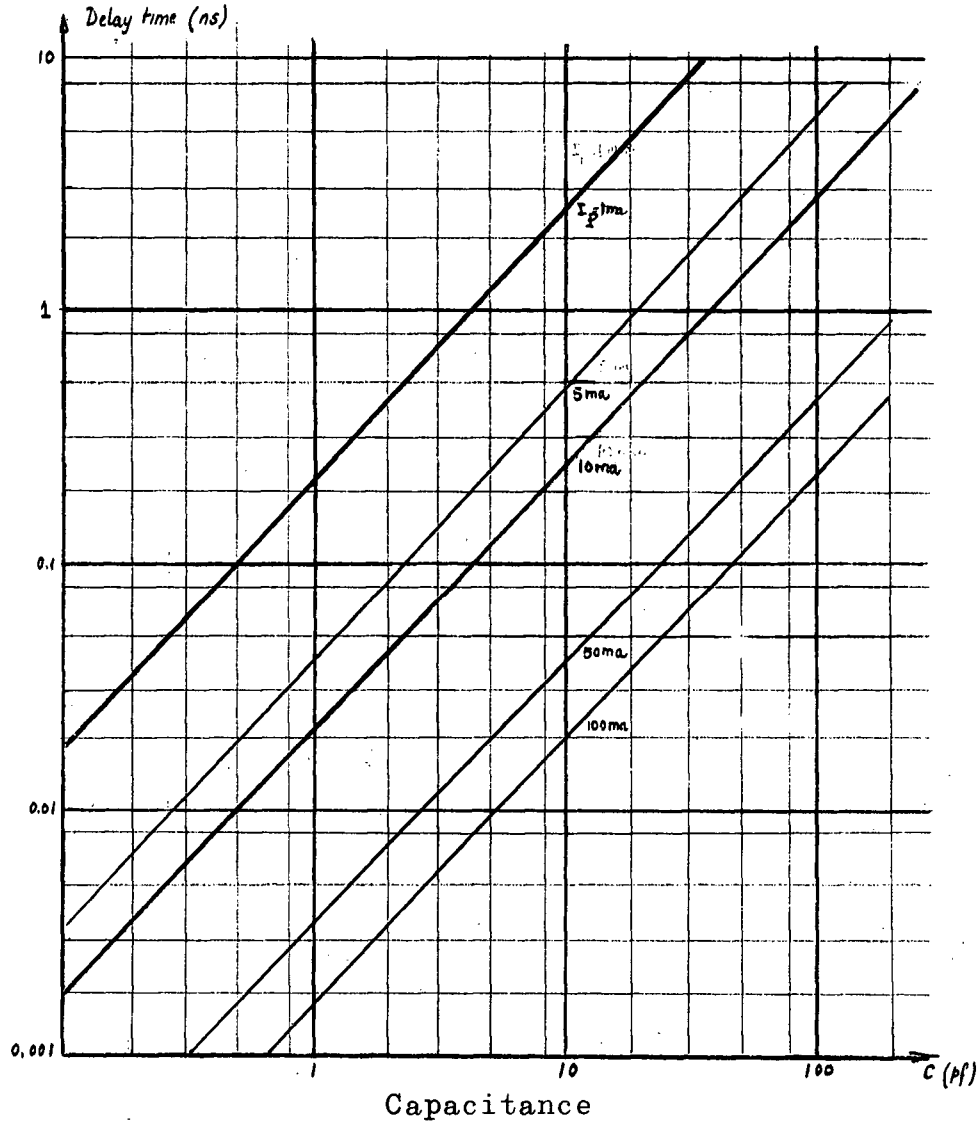

Figure 3-5. Timing Delay as a Function of Tunnel Diode Capacitance and Peak Current.

Case II: Voltage Bias

In this case, both R and L were assumed finite and equations 3-5 and 3-6 were solved for various values of R and L. Switching was accomplished by the application of a positive trigger voltage defined here as a modified step-function (0.5 ns rise time) voltage source in series with the d-c power supply. The voltage v(t) across the diode was found to exhibit the same general behaviour as for the current-bias case. The inductance was found to affect the switching time and delay time and, to a smaller extent, the rise time. Figure 3-6 shows the dynamic v-i behaviour for various values of L. It is seen that the dynamic v-i curve follows the load line only for L = 1 nh. (nh = nanohenry = 10^{-9} henry). The larger values of inductance increase the delay time and, therefore, the switching time by an appreciable amount.

It should be noted that the capacitance was assumed constant throughout the analysis. This is a valid assumption since it was found that taking the capacitance variation into account had negligible effect on the switching time.

3.3 Approximate Formula for the Rise Time of a Tunnel Diode.

An approximate formula for the rise time can be easily derived under the following assumptions:

1. The load line is assumed horizontal and tangent to the peak of the characteristic.
2. The v-i characteristic of the diode is linearized.

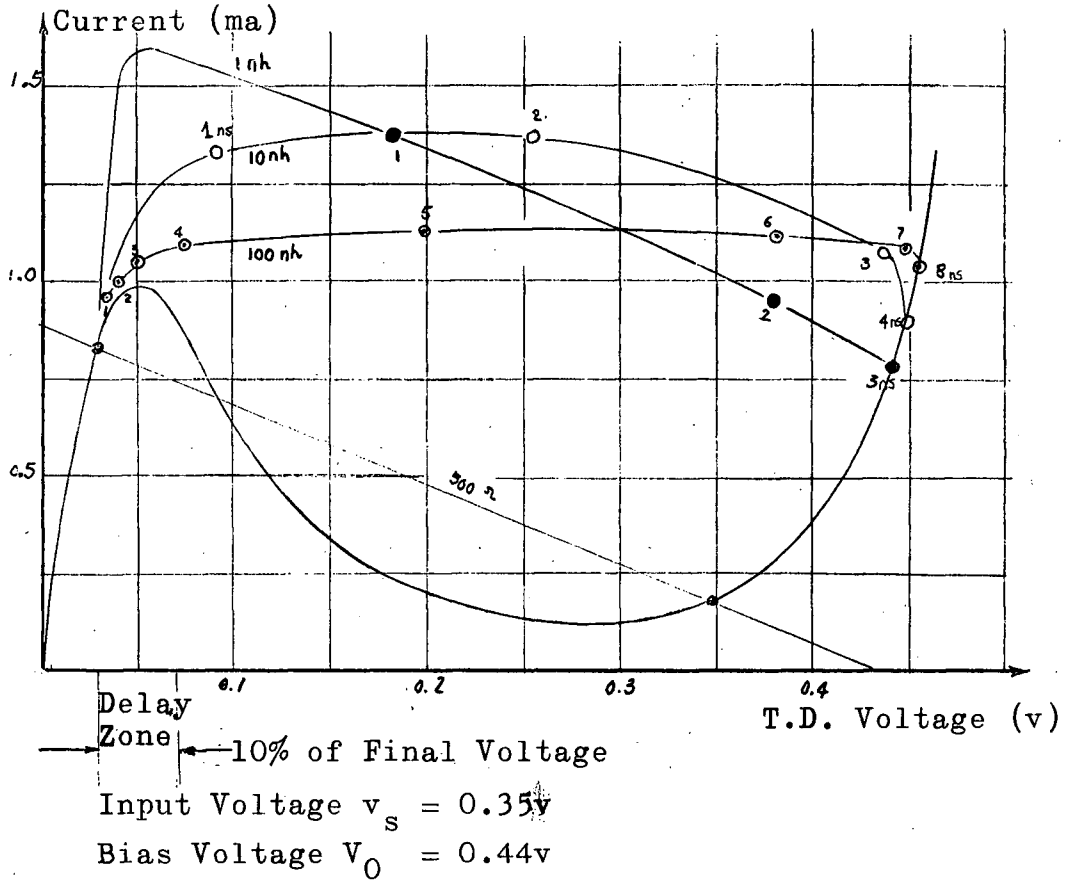

Figure 3-6. Dynamic v-i Transient Behaviour for L = 1, 10 and 100 nh. (C = 10 pf, I_P = 1 ma, R_V = 500 ohms).

From equation 3-10 we have:

$$i_c = C \frac{dv}{dt} \quad ;$$

for switching we have:

$$i_c \cong C \frac{\Delta V}{\tau} \qquad \text{where } \tau \text{ is the rise time,}$$

and $$i_c \cong I_P - I_V$$

$$\Delta V \cong V_F - V_P$$

$$\therefore \qquad \tau \cong C \frac{(V_F - V_P)}{(I_P - I_V)} = \frac{C}{I_P}\left[\frac{V_F - V_P}{1 - \frac{I_V}{I_P}}\right] \qquad \ldots(3\text{-}11)$$

This equation shows the dependence of the rise time on the figure of merit, the forward voltage, and the peak to valley current ratio.

3.4 Experimental Results.

The experimental circuit used to test the switching time of tunnel diodes is shown in Figure 3-7. All the resistors used were high-frequency non-inductive resistors and the whole circuit was built in a coaxial form.

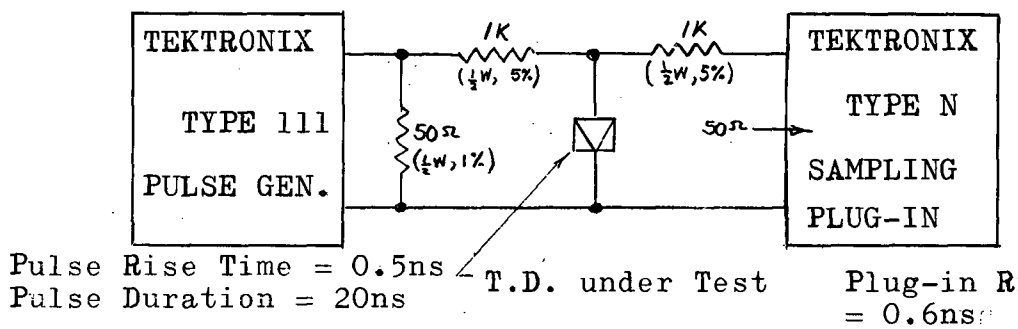

Figure 3-7. Tunnel Diode Switching Test Circuit.

Figure 3-8 shows the waveforms obtained for a T1925 (I_P = 1 ma, C_V = 10 pf) tunnel diode using the switching test circuit. To illustrate the delay between input and output: one of the input signals (waveform 1) as seen across the output

terminals with the diode open-circuited, was superimposed on the output waveforms 2 and 3 obtained with the diode in the circuit. These output waveforms were obtained for current overdrives of 20% and 40% respectively, and were displayed using a Tektronix type N sampling plug-in. The input signal corresponds to the 20% overdrive case. The rise time of the sampling plug-in is 0.6 ns and should be accounted for in the measurement, since the total rise time is the square root of the sum of the squares of the scope and circuit rise times.

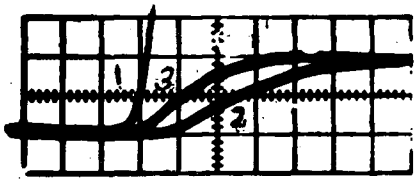

Figure 3-8. Experimental Switching Waveforms (1 ns/div horizontal, 10 mv/div vertical)

(1) Input Voltage, for 20% Overdrive
(2) Output Voltage, for 20% Overdrive
(3) Output Voltage, for 40% Overdrive.

The displayed rise times are of the order of 3.5 ns. This agrees fairly well with the values predicted from the computer solutions, and the value given by the approximate formula in equations 3-11.

3.5 Summary.

1. The switching time of the tunnel diode consists of

a delay time and rise time. Ignoring the effect of series inductance, the delay time is dependent on the figure of merit and on the current overdrive; the rise time is dependent on the figure of merit and, to a smaller extent, on the overdrive.

2. A large series inductance in the circuit increases the delay time and changes the dynamic v-i path considerably (voltage bias case).

3. For a given semiconductor, the figure of merit is dependent on the doping concentration: the higher the doping the better the figure of merit.

4. For a given level of doping, the figure of merit is dependent on the energy gap, the dielectric constant, and the reduced mass of the electron. Semiconductors with small energy gaps, dielectric constants, and reduced masses have the best figures of merit.

Though the preceding analysis is based on the Ge tunnel diode, it can be extended with minor modifications to other materials.

4. STATIC AND DYNAMIC CHARACTERISTICS OF SERIES-CONNECTED TUNNEL DIODES

When a number of tunnel diodes are connected in series with a common source, a multistable voltage-current composite characteristic is obtained. The form and complexity of the characteristic will depend on the individual elements.[29] Attention will be confined to the most interesting combination,[2] which results in 2^n stable states generated using n negative resistance elements, provided the individual elements obey certain rules derived in the following sections.

As a first step, a study of the static characteristic of such a composite device was undertaken to establish the relationship that the static parameters of the individual elements must satisfy. Experimental curves, obtained using tunnel diodes in series, were found consistent with the established relationships.

Because of the impossibility of making accurate physical measurements of the circuit current and voltages at high frequency, and the difficulty of a purely analytical approach, a computer solution of the circuit equations was carried out. The computer solution led to a better understanding of the circuit operation.

4.1 Static Characteristic of Two Tunnel Diodes in Series.

Simple graphical constructions based on the individual device characteristic-curve enable one to predict the nature of

the composite characteristics.

Figure 4-1 shows the linearized characteristic curve of a typical tunnel diode. For the purpose of the following discussion, the range $0 < v < V_P$ is defined as a "0" or "low voltage" state, and the range $V_1 < v < V_F$ is defined as a "1" or "high voltage" state. The negative resistance region $V_P < v < V_1$ is not counted as a state since it is unstable in most cases.

Multistable composite characteristics are obtained when the tunnel diodes have progressively overlapping multivalued ranges and are constrained to have the multivalued quantity (current) the same at every instant of time. To illustrate the composite characteristics, we consider the case of two tunnel diodes connected in series and driven from a low impedance source. Let

$$I_{P2} > I_{P1} \qquad \ldots(4\text{-}1)$$

$$I_{V1} > I_{V2} \qquad \ldots(4\text{-}2)$$

$$V_{F2} > V_{F1} \qquad \ldots(4\text{-}3)$$

Figure 4-2(a) shows the linearized individual tunnel diode characteristics (in this Figure $V_{F2} = 2\ V_{F1}$). Figure 4-2(b), the piecewise linear composite characteristic, was obtained using the fact that at any point the current is identical in both diodes while the terminal voltage is the sum of the voltages across each. Inspection of the superimposed individual characteristics reveals which portions overlap in current. Each

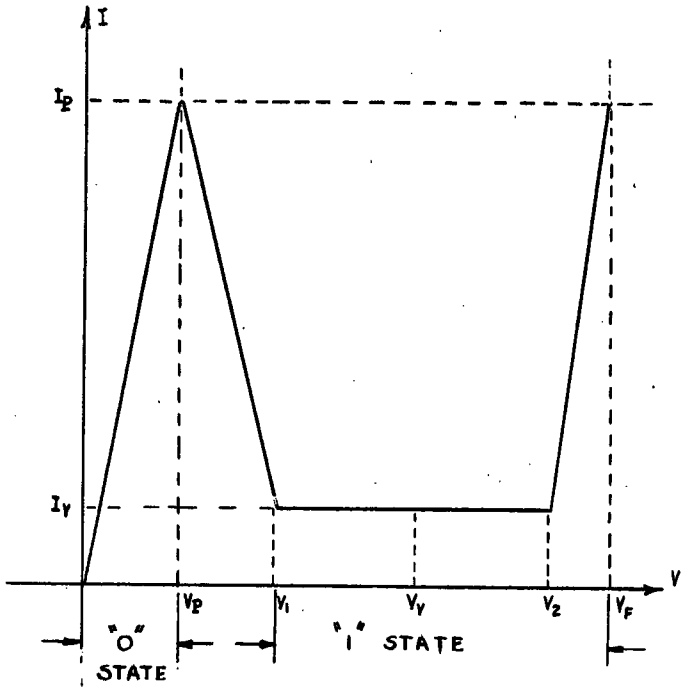

Figure 4-1. Linearized Characteristic Curve of a Tunnel Diode.

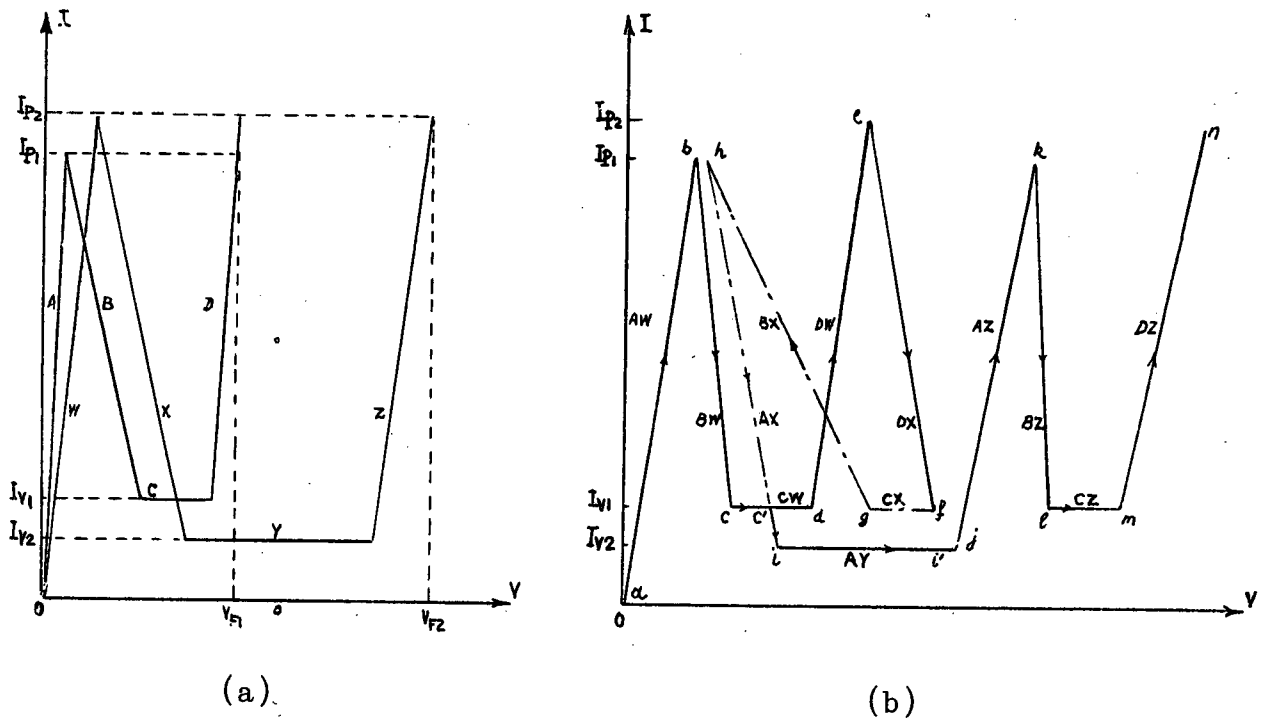

Figure 4-2(a) Tunnel Diodes Individual Characteristics
(b) Composite Characteristic.

part of an individual characteristic combines with every part of the other, having current values in common with it, to form a linear segment in the composite characteristic.

In the following discussion, the various stable states will be assigned a binary notation. When assigning a pair of binary digits to a state, the digit to the right (the less significant digit) will refer to the first tunnel diode D_1, and the digit to the left (the more significant digit) will refer to the second tunnel diode D_2. Later as more diodes are added, the sequence will be preserved with the least significant bit to the extreme right.

Referring to Figure 4-2(b), a short discussion of the composite characteristic, its stable states, and the order in which they are generated, will lead to a better understanding of the circuit behaviour.

00 State:

Initially both diodes are in their low voltage state. As the applied voltage is increased, the current and voltage across the diodes increase until the current reaches the value of I_{P1}. This is the first peak of the combined characteristic. Segment AW is given a 00 binary representation.

01 State:

As the input voltage increases, the current decreases forcing the voltage across D_1 to increase and that across D_2 to decrease (since $I_{P2} > I_{P1}$). Hence, D_2 remains in its low voltage state while D_1 switches to its high voltage state and segments BW, CW, DW are traced. The binary representation of CW and DW is 01.

10 State:

If the voltage is increased further, the current and voltage in both diodes increase until I_{P2} is reached (second peak of the composite characteristic). Beyond this point, increasing the voltage must result in a decrease in current through the diodes. Along segment DX the voltage across D_2 increases but that across D_1 decreases until point "f" is reached. The system then switches to point "i'" for an infinitesimal voltage increase via the virtual path "fghii'". This path is the unique path from "f" to "i'", having the property of identical current across the diodes at all points. However, over this path the voltage is always less than it is at "f". It is clear that in the switching process the excess voltage must be taken up by a storage element[2] (in this case the tunnel diode capacitance). During this process, the current decreases to the low value of I_{V2}; diode D_2 ends up in its high-voltage state while diode D_1 is switched back to its low-voltage state because D_1 cannot support the low value of I_{V2} unless it is near its zero voltage level. Further increase in voltage generates segments AY and AZ with a binary representation of 10.

11 State:

As the current reaches again the value I_{P1}, the third peak of the composite characteristic is brought forth. For any applied voltage beyond this, tunnel diode D_2 remains in the high voltage state while the voltage across D_1 increases and segments BZ, CZ and DZ are traced. CZ and DZ have the binary representation 11.

The above discussion is valid only for increasing applied voltage. If the process is reversed, the path traced in coming back is "nmlkjic'cba". The binary state 01 is missing in this case, showing an irreversible effect exhibited by the characteristic.

4.2 Static Characteristics of n Tunnel Diodes.

The results of the preceding section can be extended to n elements of the type discussed by generalizing conditions 4-1, 4-2, 4-3 to become:

$$I_{Pn} > I_{P(n-1)} \cdots > I_{P1} \qquad \ldots(4\text{-}4)$$

This condition states that the n^{th} tunnel diode cannot switch to its "1" state until all the preceding (n-1) tunnel diodes are in their "1" state.

$$I_{Vn} < I_{V(n-1)} \cdots < I_{V1} \qquad \ldots(4\text{-}5)$$

When a tunnel diode switches to its "1" state it obviously must pass through its valley. Then condition 4-5 ensures that it will cause all lower order diodes (which must be in the "1" state from 4-4) to switch back to the zero state. For the binary regions to have equal voltage ranges the requirement is:

$$V_{Fm} = 2^{m-1} \; V_{F1} \quad \text{for } m = 2 \text{ to } n \qquad \ldots(4\text{-}6)$$

Also for all binary states to be distinct:

$$V_{V1} < V_{Fn} - \sum_{m=1}^{n-1} V_{Fm} \qquad \ldots(4\text{-}7)$$

The above conditions(*) ensure the existence of 2^n distinguishable positive regions derived from n tunnel diodes. In a special case resulting from relaxation of conditions 4-6 and 4-7, (n+1) stable positive regions can be generated using n devices; this case arises from the use of diodes satisfying conditions 4-4 and 4-5 and having identical voltage characteristics. By altering the four conditions, either singly or together, it is possible to achieve certain numbers of positive resistance regions between (n+1) and 2^n.

4.3 Experimental Results.

A curve tracer[16] was used to obtain the static characteristics of series-connected tunnel diodes. The following features incorporated in the curve tracer were essential to minimize the possible oscillations in the negative resistance region:

1. a low series resistance sweep circuit,
2. a low inductance diode test mount.

Referring to Table 2.1, it is seen that a combination of GaAs, Ge, InAs, and InSb diodes can be made to satisfy condition 4-6 approximately. However, at the time of this

(*) These conditions are similar to the ones obtained by Rabinovici and Renton[2] for n current controlled negative resistance devices.

writing, the InAs and InSb diodes were not yet commercially available and their characteristic v-i curve had to be simulated. The parallel combination of a Ge tunnel diode and an ordinary Ge diode simulates the InAs diode with a forward voltage $V_F = 0.275$v. The parallel combination of a Ge tunnel diode and a Silicon backward diode(*) simulates the InSb diode with a forward voltage $V_F = 0.15$v.

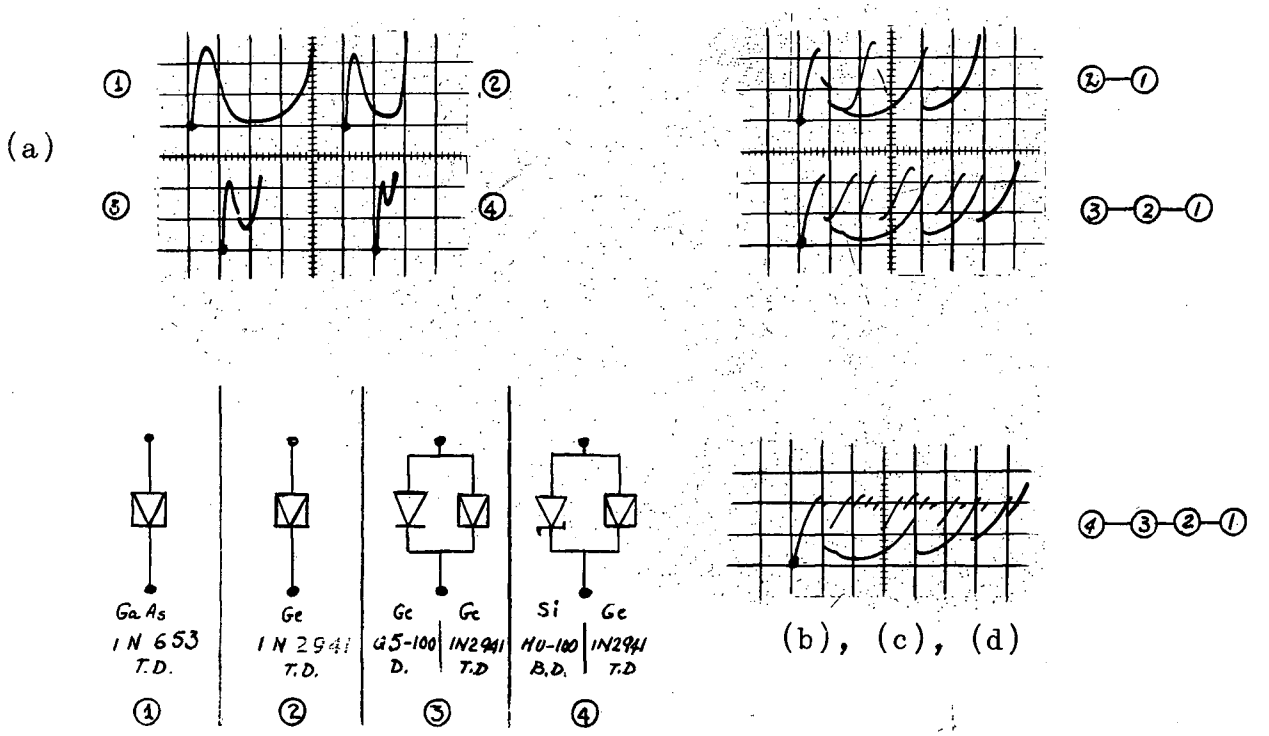

Figure 4.3(a) Experimental Characteristics of the Negative Resistance Elements
(b) Two Elements Composite Characteristic
(c) Three Elements Composite Characteristic
(d) Four Elements Composite Characteristic
(2.3 ma/div vertical; 0.25 v/div horizontal).

(*) The backward diode is a tunnel diode, with a relatively low impurity concentration. It is used with reverse applied voltage and exhibits, over that range, characteristics similar to those of a Zener reference diode but with a lower voltage drop. The voltage drop is 0.28v for Si and 0.08v for Ge backward diodes.

Figure 4-3(a) shows the separate individual characteristics (satisfying conditions 4-5, 4-6, 4-7, and 4-8) of four negative resistance elements, and the diodes used to obtain these characteristics. Figures 4-3(b), (c), and (d), show the composite characteristics having 4, 8, and 16 stable positive regions; these characteristics were obtained using two, three, and four devices respectively. A 32 state composite characteristic could be obtained by the addition of a fifth element consisting of the parallel combination of a Ge tunnel diode and a Ge backward diode. This combination would have a forward voltage of 0.08v.

4.4 Dynamic Characteristics.

The study of the static characteristics established the necessary conditions for the realization of 2^n stable states for n tunnel diodes. These conditions hold when voltage and current variations occur at speeds well below the switching speed of the device.

However, at high frequencies, the effects of storage and stray elements associated with the device must be taken into consideration;[30],[31] and the conditions derived from static considerations become necessary but not sufficient for proper operation. It is the purpose of the following investigation to:

(1) determine the exact influence of the circuit parameters on the response,

(2) formulate some empirical conditions which will ensure correct operation and fast response.

Most of the investigation was carried out by computer solution of the circuit equations. Only a two tunnel diode circuit was investigated and the results generalized wherever possible.

4.5 Two Tunnel Diode Multistate Circuit.

The circuit investigated is shown in Figure 4-4(a) and its equivalent circuit in Figure 4-4(b). With minor alterations, this circuit could represent a full binary adder, a two-bit analog-to-digital converter or a counter. It consists of a Ge (1N2941) and a GaAs (1N653) tunnel diode in series. The static characteristics of the individual diodes satisfy the conditions derived in section 4.2. The diodes are biased from a constant current source I_0; where $I_{P1} > I_0 > I_{V1}$. The triggering source v_s is an ideal voltage source. The load line resistance R is chosen to be slightly larger than the magnitude of the larger of the two negative resistances of the diodes (see Appendix III). This choice ensures that:

(a) R is small enough for all the stable operating points to be accessible, and

(b) the negative resistance regions of the composite characteristic are unstable.

If v_1 and v_2 are the voltage drops across the first and second diode respectively (neglecting series resistance), and i is the instantaneous current, then the equations describing the behaviour of the circuit are:

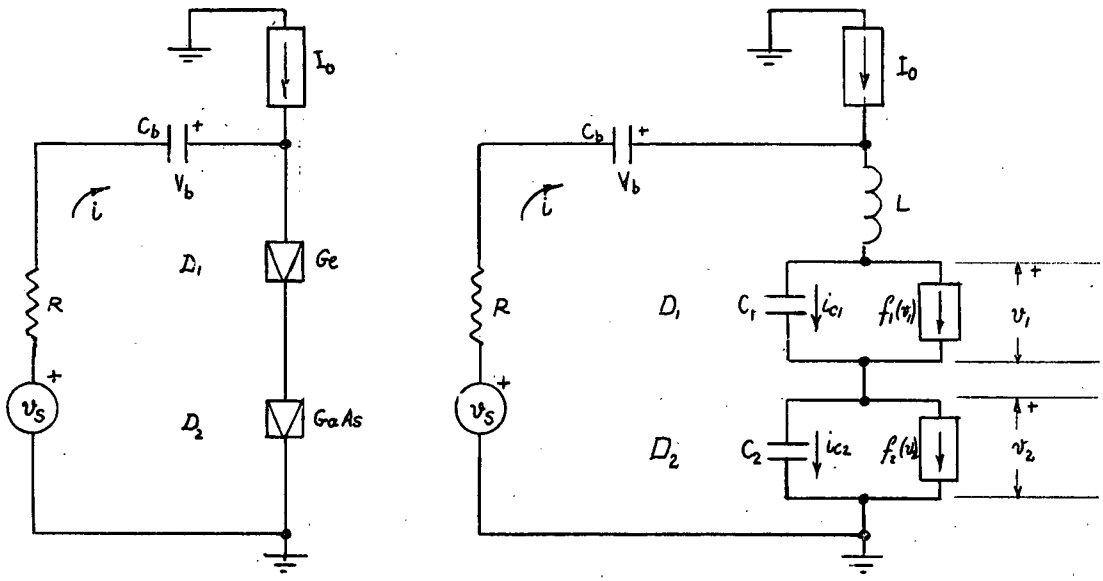

(a) (b)

Figure 4-4. Two Tunnel Diode Multistate Circuit.

$$L \frac{di}{dt} = E - Ri - v_1 - v_2 \qquad \ldots(4\text{-}8)$$

$$C_k \frac{dv_k}{dt} = (i + I_0) - f_k (v_k) \quad k = 1, 2 \qquad \ldots(4\text{-}9)$$

$$i_{ck} = (i + I_0) - f_k (v_k) \quad k = 1, 2 \qquad \ldots(4\text{-}10)$$

where L = total inductance in the circuit,

$E = V_b + v_s$,

V_b = voltage across the blocking capacitor C_b (C_b is assumed a short circuit at the frequencies of interest),

i_{ck} = capacitive current, and

$f_1(v_1)$, $f_2(v_2)$ are given by equations AII-3 and AII-4 respectively. These equations closely approximate the experimental v-i characteristics of the diodes, the d-c parameters of which are given in Table 4.1. Comparison of the circuit behaviour with C_k held constant rather than variable indicated only trivial differences. Consequently most of the computation was carried out with C_k constant. It should be noted that equations 4-8 and 4-9 are invariant to the substitutions given in equations 3-8 and 3-9.

	I_P ma	I_V ma	V_P v	V_V v	V_F v	|r| ohms	$\delta I_V = I_{V1} - I_{V2}$ ma
Diode D_1 Ge 1N2941	4.56	1.16	0.06	0.3	0.48	30	0.82
Diode D_2 GaAs 1N653	4.86	0.34	0.10	0.6	1.0	40	

Table 4.1 D-C Parameters of the Two Diodes

4.6 Switching Behaviour.

The tunnel diodes' switching behaviour, under the application of modified step voltages with 0.5 ns rise time, was investigated. Three input voltages of amplitudes 0.45, 0.90 and 1.35v, cause the diodes to switch from the 00 state to the 01, 10, and 11 states respectively. The superimposed static and dynamic v-i characteristics of the two diodes are shown in Figures 4-5(a), 4-6(a) and 4-7(a). The parameters of the circuit under investigation are also listed in these Figures. In this initial study, the inductance L was assumed zero. This simplifies

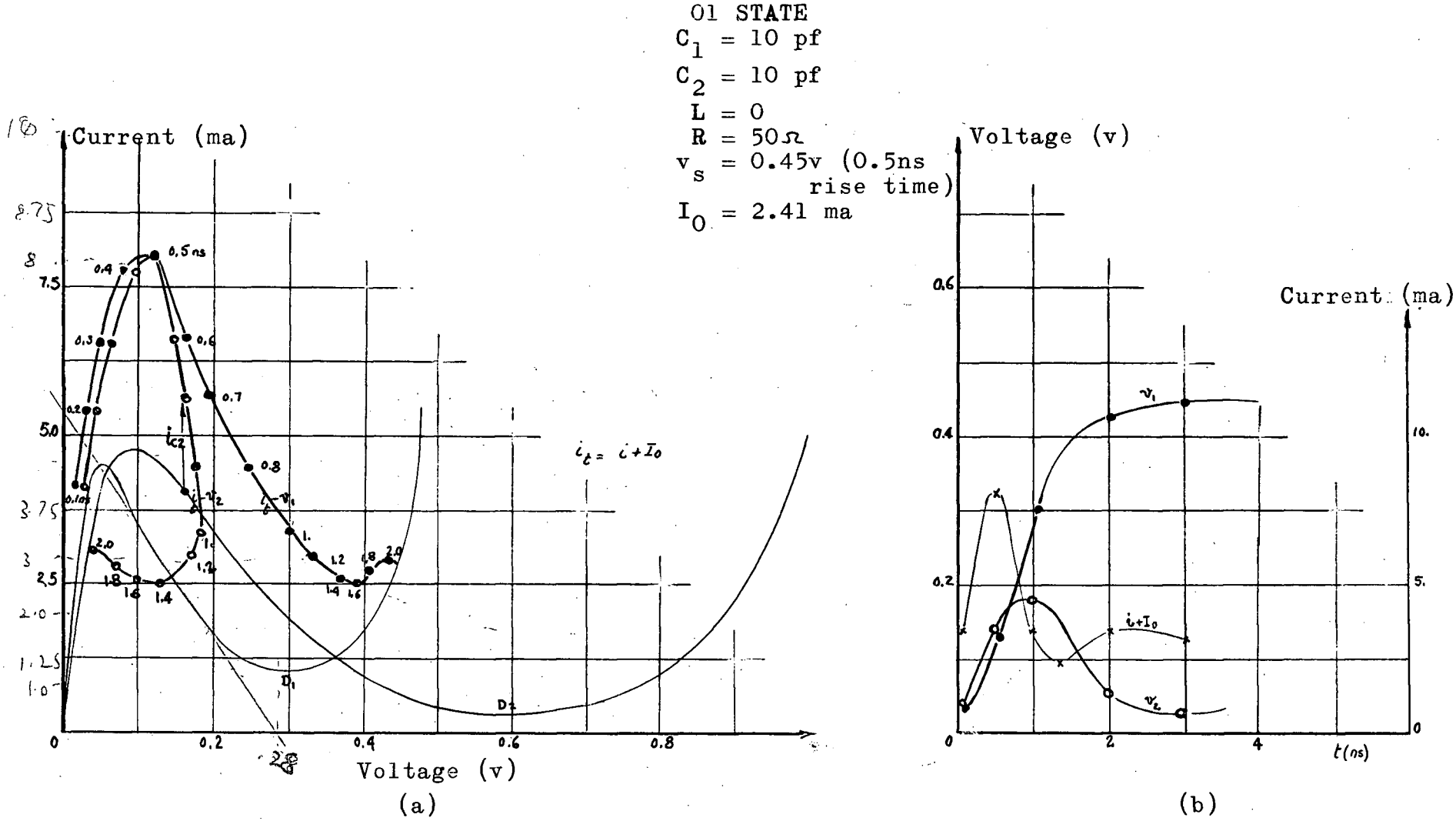

Figure 4-5(a) Dynamic v-i Characteristics of the Multistate Circuit (00—01)
(b) Voltage and Current Waveforms (00—01).

the solution, cuts down on computation time and makes the behaviour of the circuit relatively easier to analyse. The effects of inductance on the switching transient will be treated in a later section.

01 State:

Initially both diodes are in their low voltage state. A trigger signal with 0.45v amplitude is applied to the circuit (see Figure 4.5(a)). During the rise time of the signal, the current and voltage across both diodes increase. When the step reaches its steady value, a transient relaxation process occurs. Both diodes switch towards their high voltage state and the series current decreases to follow the transient load line. Unbalance in the inherent switching-time constants causes the faster diode D_1 to race diode D_2 with respect to voltage increase. Eventually, diode D_1 can cause the current i to decrease to such an extent that the capacitive current i_{c2} becomes zero and the voltage across D_2 ceases to increase. Further decrease in i, discharges capacitance C_2 causing diode D_2 to switch back to its low voltage state while D_1 assumes its high voltage counterpart. The final adjustment to the quiescent condition relaxes very rapidly. A plot of the transient voltages and current versus time is shown in Figure 4-5(b).

10 State:

A trigger signal with 0.9v amplitude is applied to the circuit. When the steady state is reached, diode D_1 is in its "0" state while diode D_2 is in its "1" state. The switching

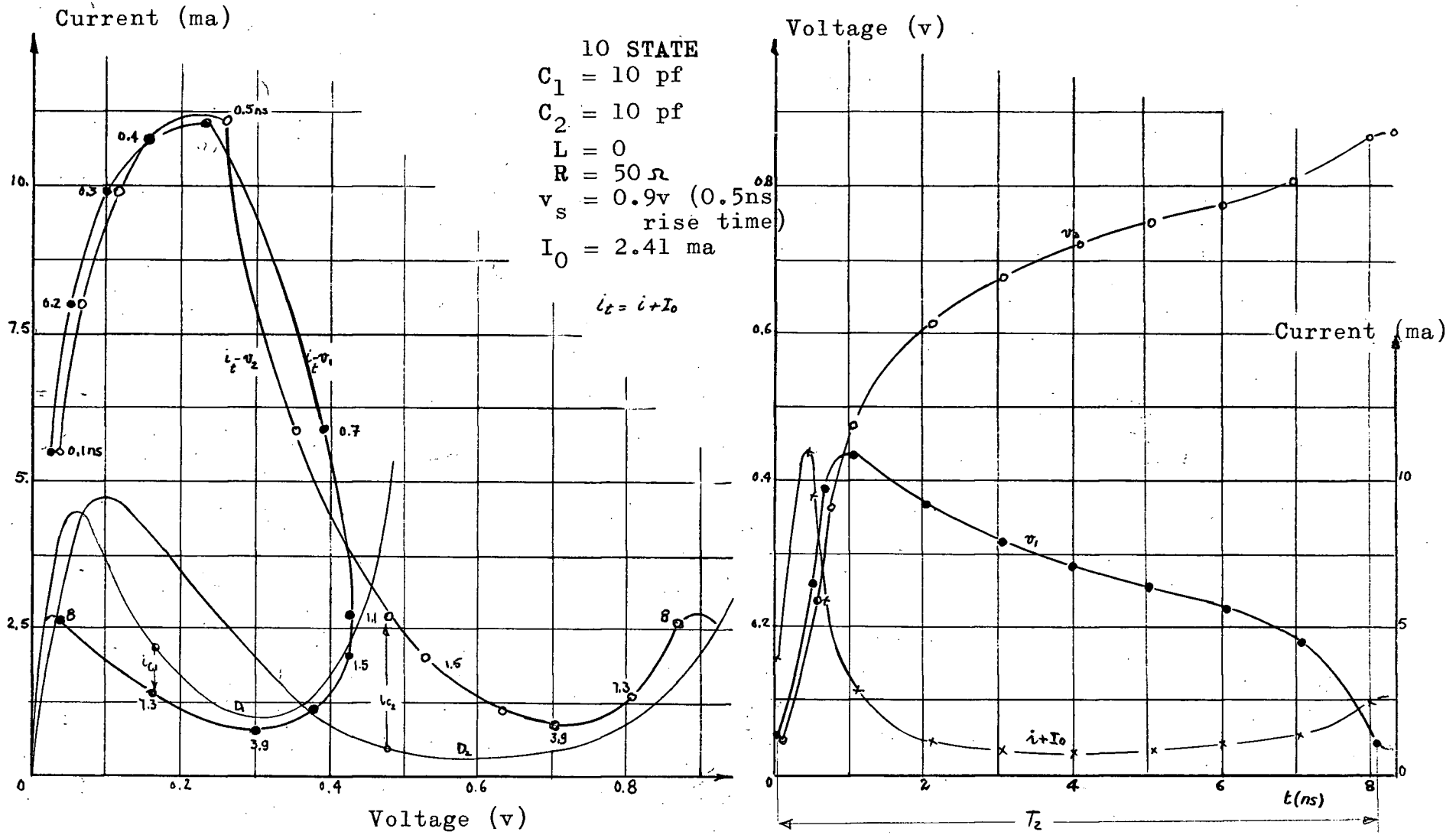

Figure 4-6(a) Dynamic v-i Characteristics of the Multistate Circuit (00—10)
(b) Voltage and Current Waveforms (00—10).

behaviour differs radically from the preceding case. When the step reaches its steady value, each diode relaxes towards its high voltage state (see Figure 4-6(a)). The current decreases until a point is reached where the capacitive current i_{c1} becomes zero and the voltage across D_1 stops increasing; this occurs when D_1 is in its high voltage state. Any further decrease in i discharges C_1 while C_2 is charged; this effect is due to the constraints established by the d-c characteristics of the diodes. Therefore diode D_1 is momentarily turned on, and then relaxes to its low voltage state, giving rise to what may be termed a "precursor"[34] pulse of duration T_2 (see Figure 4.6(b)). The portion of the relaxation process during which the dynamic operating point of D_1 traverses its valley, makes up the largest portion of T_2.

11 State:

A trigger voltage with 1.35v amplitude is applied to the circuit. In the steady state, both diodes end up in their high voltage state. Quiescent conditions are reached more rapidly than in the previous two cases. Figure 4-7(a) and Figure 4-7(b) show the dynamic behaviour and the current and voltages as a function of time for this particular case.

From the above discussion and the transient waveforms, it is obvious that the duration of the precursor pulse T_2 can be considered as a measure of the speed of operation of the circuit. For the case considered here, the steady states corresponding to all the output possibilities can be achieved in $T_2 = 8$ ms.

4.7 Effect of Capacitance on Transient Behaviour.

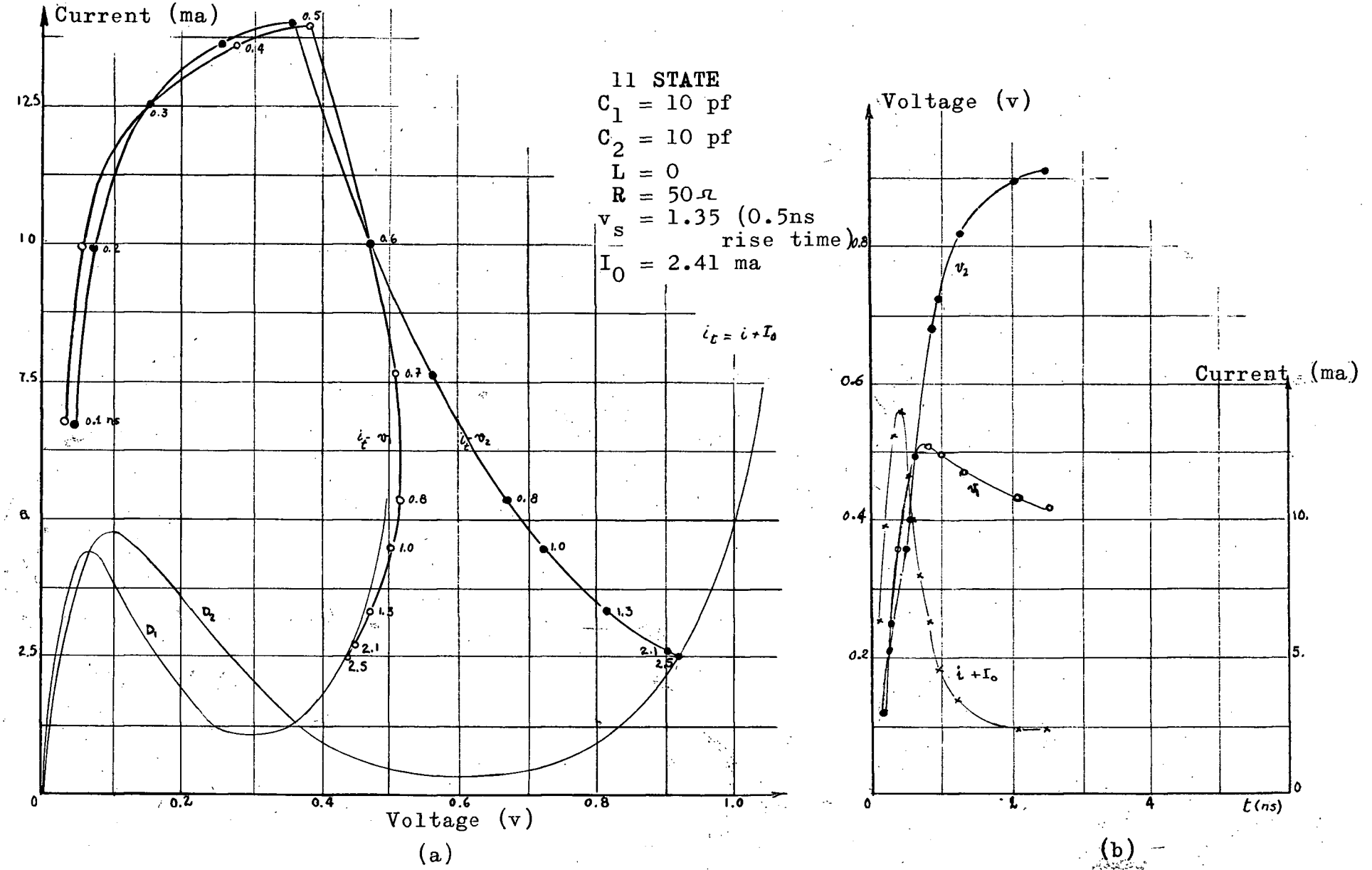

Figure 4-7(a) Dynamic v-i Characteristics of the Multistate Circuit (00—11)
(b) Voltage and Current Waveforms (00—11).

For L = 0, the switching times are dependent on the figures of merit of both diodes: the smaller the figures of merit the smaller the overall switching times. However, it was found that the capacitance ratio $C_1:C_2$ affects the switching time and the operation of the circuit. Figure 4-8 shows the transient voltage waveforms for capacitance ratios of 1:2, 1:1 and 1:0.75. The waveforms for the three states are shown; the voltage input being a step in each case.

A comparison of the waveforms shows that for a capacitance ratio of 1:2, the general response is slowed down and the duration and peak amplitude of the precursor pulse are quite large. The ratio 1:0.75 offers a better response and a reduced peak amplitude for the precursor pulse. This particular ratio corresponds to equal $C|r|$ time constants for the two diodes. Further increase in the capacitance ratio $C_1:C_2$ does not improve the response and may cause false operation. An example of false operation (waveforms not shown) is obtained when the capacitance ratio is increased to 1:0.5. In this case, an input corresponding to the 01 state, causes the circuit to end up in the 10 state; tunnel diode D_1 is switched partially on and then reset to the low voltage state while diode D_2 settles in its valley voltage region.

The above discussion suggests the use of the capacitance ratio as an additional parameter which can be adjusted in designing for fast response. The diode capacitances should be chosen as small as possible, and the diode with the smaller band gap should have the larger capacitance. Furthermore, the

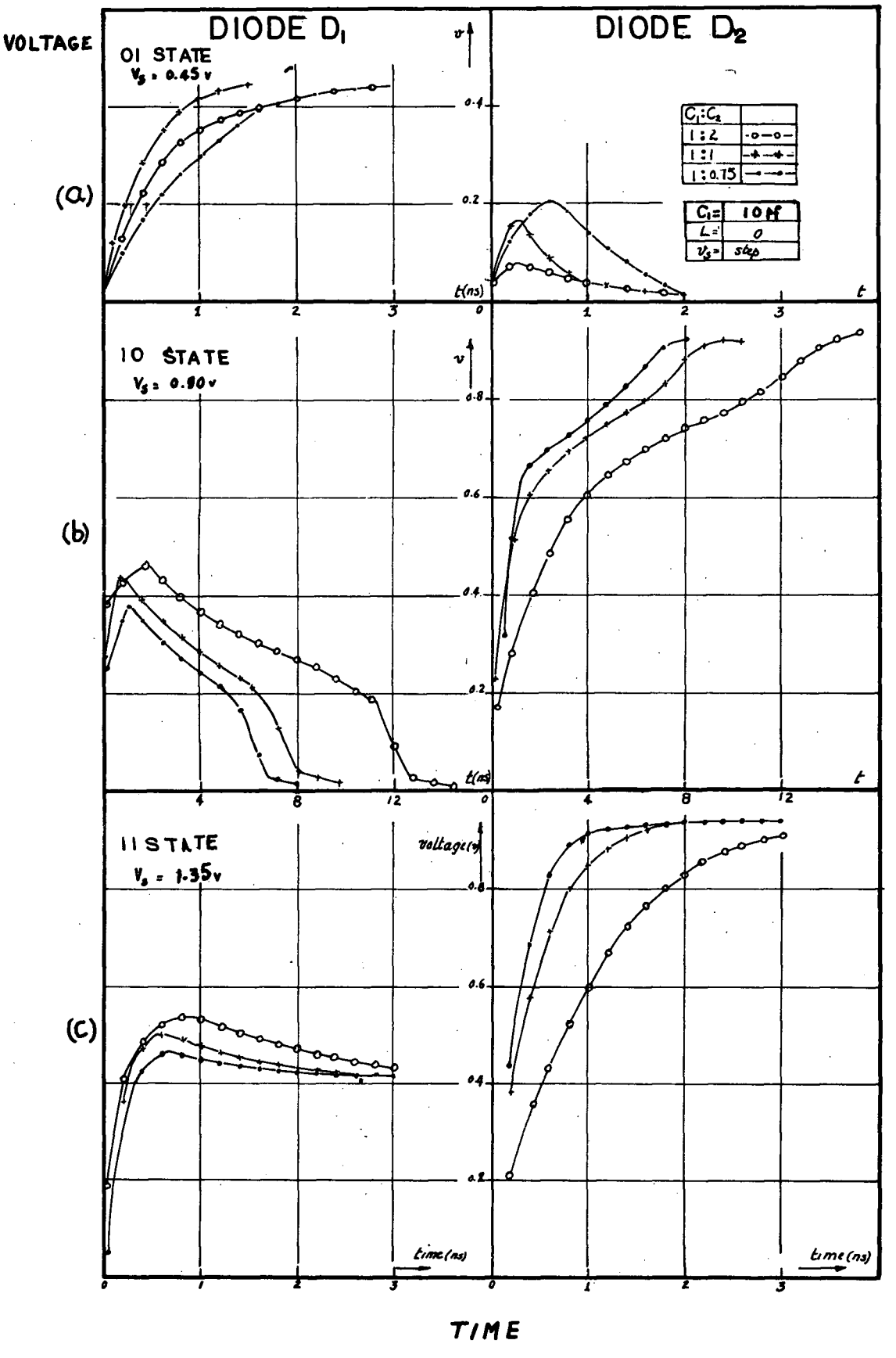

Figure 4-8. Effect of Capacitance on Transient Behaviour (R = 50 Ω)

capacitance ratio should fall in the range $1 \leqslant (C_1 : C_2) < 1.9$ for fast response and proper operation. The ratio $(C_1 : C_2) = 1 : 0.75$ (equal time constants) seems to offer optimum response.

4.8 Effect of the D-C Parameters of the Tunnel Diodes on the Switching Behaviour.

For fixed capacitances, the difference between the valley currents of the diodes $\delta I_V = (I_{V1} - I_{V2})$ determines to a great extent the duration of the precursor pulse T_2: the larger δI_V, the larger the capacitive current discharging capacitance C_1 and therefore the faster the relaxation transient towards a stable state. To show the effect of δI_V on the duration of T_2, the Ge diode v-i characteristic used in the preceding analysis was replaced by a new characteristic identical to the first, but with a valley current of 0.656 ma i.e., δI_V was reduced from 0.82 ma to 0.32 ma. This reduction in δI_V increased the precursor pulse duration to 19 ns (it was previously 8 ns; see Figure 4-8(b) for the case $C_1 = C_2 = 10$ pf). Figure 4-9 shows the dynamic v-i characteristic for the 10 state with $\delta I_V = 0.32$ ma. The change in δI_V did not affect the values of the switching time for the 01 and 11 states by any appreciable amount.

The difference between the peak currents of the two diodes is not critical as far as switching time or proper operation is concerned, however, it is well worth mentioning that the larger the I_P/I_V ratio for each individual diode, the faster the circuit response.

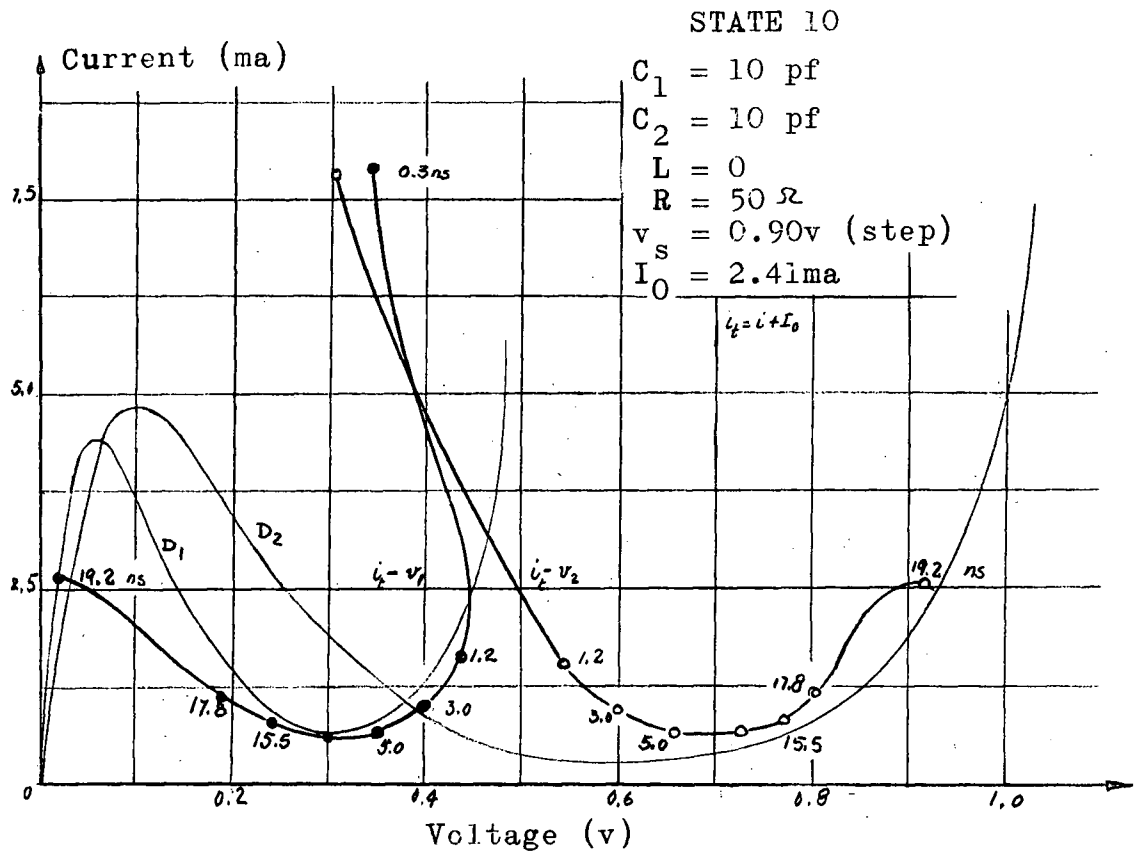

Figure 4-9. Dynamic v-i Characteristic for δI_V = 0.32 ma (R = 50Ω).

The effects of V_P, V_V, V_F on the switching behaviour were not investigated since these voltages were assumed to be fixed for a given semiconductor material.

4.9 Effect of Inductance on Transient Behaviour.

Only small values of inductance were considered in this investigation. Figure 4-10 shows the output voltage waveforms for two values of inductance: 10 and 30 nh. With the low resistance load lines and large input voltages encountered in the multistate circuit, the main effects of inductance on the switching behaviour are:

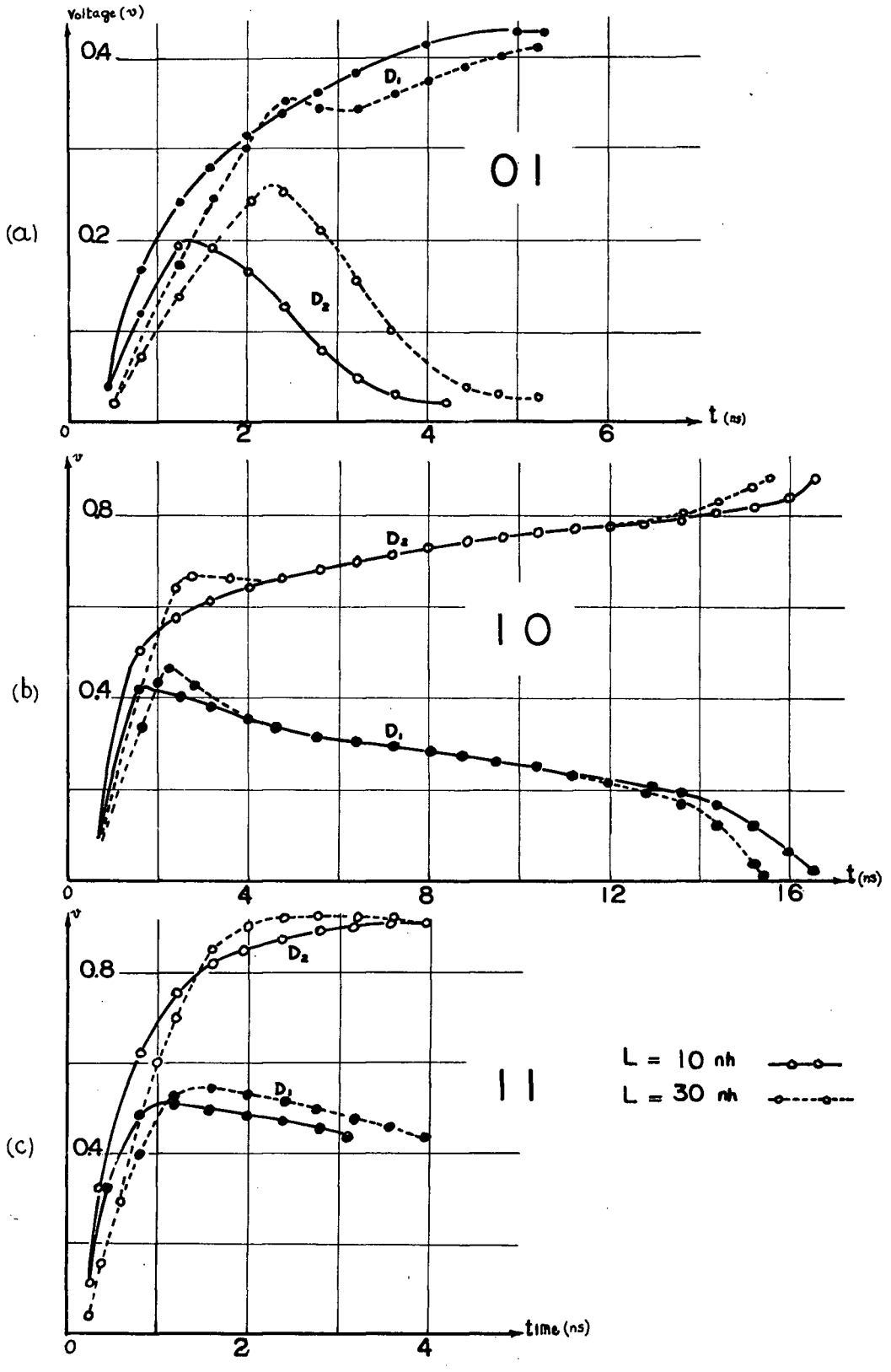

Figure 4-10. Effect of Inductance on Transient Behaviour

$C_1 = 14.4(1 - \frac{v}{0.6})^{-\frac{1}{2}}$pf; $C_2 = 14.4(1 - \frac{v}{1.2})^{-\frac{1}{2}}$pf; R = 50 Ω,

v_s(0.5ns r.t.) = 0.45, 0.90, 1.35v respectively for 01,10,11 states.

1. The inductance introduces a small delay in the output voltage waveform.
2. The higher value of inductance (30 nh) causes an overshoot in the initial rise of the voltage waveform. This overshoot decays in a damped oscillatory manner towards the steady state. This is shown in Figures 4-10(a), 4-10(b).
3. The higher value of inductance causes a faster relaxation of the diode transient towards its stable state. This shortens the duration of the precursor pulse and increases the speed of operation (see Figure 4-10(b)).

Hence, by proper choice of the inductance and load line resistance, the inductive transient can be made to contribute relatively flat top output waveforms, and to speed up the circuit operation.

4.10 Effect of Input Pulse Rise Time on Transient Behaviour.

The behaviour of the circuit for input steps with 3, 5, 10 ns rise time was investigated. The following observations were made:

1. The dynamic v-i characteristics in all cases are quite similar to those shown in Figures 4-5(a), 4-6(a), 4-7(a) except for the fact that the slower the pulse rise time, the closer is the dynamic path to the d-c characteristics of the diodes, i.e., the smaller the

capacitive currents.

2. The duration of the precursor pulse is to a large extent independent of the rise time.
3. Over the positive resistance regions, the instantaneous dynamic operating point follows the input pulse rise time.
4. Over the negative resistance regions, the diodes switch, and the switching speed depends mainly on the $C|r|$ time constant and the capacitive current; the latter depends on the rise time.

4.11 Effect of Temperature on the Circuit Operation.

Table 4.2 gives the temperature coefficients of the important d-c parameters for the Ge and GaAs tunnel diodes.

From this table and the discussion in section 4.8 it is obvious that the difference in the valley-current temperature coefficients will seriously affect the switching speed. It was estimated that a change of $\pm$ 25°C in temperature produces a corresponding change of $\pm$ 15% in switching speed (T_2).

The difference in the forward-voltage temperature coefficients will affect both the switching time and the stable steady states; however, this effect is not very critical. Similarily, the difference in peak-voltage coefficients does not affect the operation of the circuit to any appreciable extent.

Hence, in choosing tunnel diodes for application in a multistate circuit, it is advisable to pick diodes having the same valley-current temperature coefficients.

Coefficient	Symbol	Germanium (1N2941)	Gallium Arsenide (1N653)
Peak Point voltage Temp. Coeff. **	$\Delta V_P/\Delta T$	-60 $\mu V/^oC$	-120 $\mu V/^oC$
Valley Point voltage Temp. Coeff. **	$\Delta V_V/\Delta T$	-1 mv/^oC	-1 mv/^oC
Forward Point voltage Temp. Coeff. **	$\Delta V_F/\Delta T$	-1 mv/^oC	-1.5 mv/^oC
Valley Point current Temp. Coeff. *	$\frac{\Delta I_V}{I_V \Delta T}\%$	0.75%/^oC	0.6%/^oC

$\Delta T = T - T_R$

* Measured

** Manufacturer's Data

T = operating temperature

T_R = room temperature

Table 4.2 Temperature Coefficients of the D-C Parameters for the Ge and GaAs Tunnel Diodes

4.12 Extension to Three Tunnel Diodes in Series.

If three tunnel diodes are connected in series, eight stable states result (see section 4.3). Table 4.3 gives the eight states of the composite device in terms of the individual diode's states.

State	D_3	D_2	D_1
1	0	0	0
2	0	0	1
3	0	1	0
4	0	1	1
5	1	0	0
6	1	0	1
7	1	1	0
8	1	1	1

Table 4.3 Stable States for Three Tunnel Diode Device

It is seen that for every state except 5, the switching process involves only two tunnel diodes and therefore the preceding analysis can be used to obtain an estimate of the switching time. For state 5, the third tunnel diode switches to its "1" state and forces the two preceding diodes to switch back to their "0" state. The switching behaviour is complicated in this case and the duration of the relaxation transients for diodes D_1 and D_2 will determine to a certain extent the speed of operation of the circuit (see section 4.13).

4.13 Experimental Results.

Figure 4-11 shows the experimental response of the circuit of Figure 4-4 to the application of pulses of amplitudes 0.45, 0.90 and 1.35v. The pulses were obtained from a Tektronix

111 pulse generator and have a rise time of 0.5 ns, a fall time of 1 ns, and a duration of 20 ns. The response was observed on a Tektronix 581 oscilloscope (rise time 3.3 ns). The parameters of the experimental circuit (C_{V1} = 20 pf, C_{V2} = 18 pf, R = 50 ohms) were approximately the same as those of the circuit analysed on the computer in section 4.9 (waveforms of Figure 4-10). No attempt was made to evaluate the inductance in the experimental circuit. The experimental results (taking into account the rise time of the oscilloscope) show relatively good agreement with the computer solutions. The duration of the precursor pulse shown is approximately 12.5 ns; this would limit the possible pulse repetition rate to 80 Mc/s.

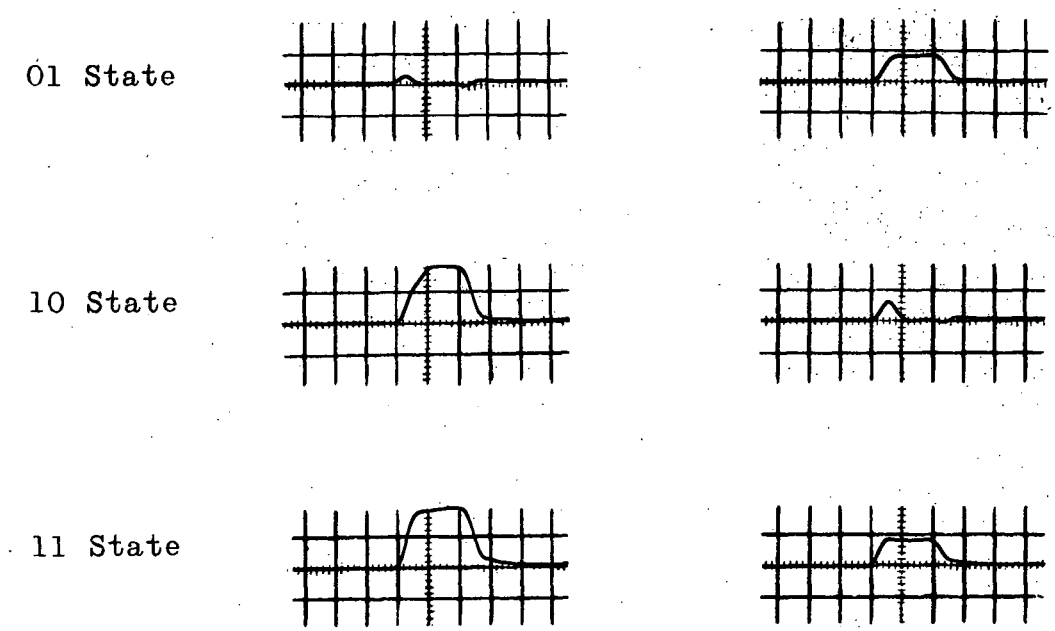

Figure 4-11. Experimental Voltage Waveforms for Two Tunnel Diode Circuit

(0.5 v/div vertical; 10 ns/div horizontal)

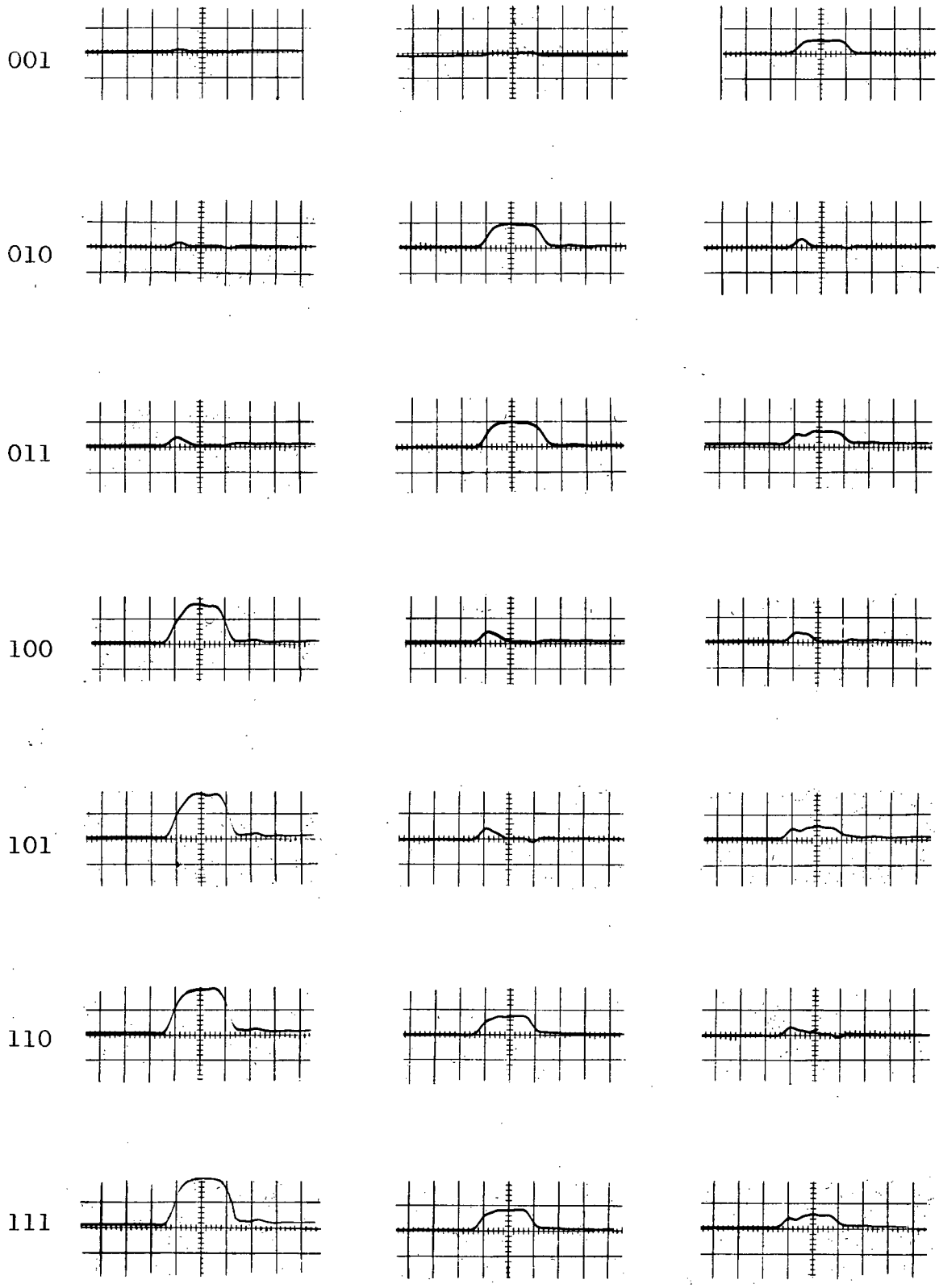

Figure 4-12. Experimental Voltage Waveforms for a Three Tunnel Diode Circuit (0.5 v/div vertical; 10ns/div horizontal)

Figure 4-12 shows the response of the eight state circuit (see sections 4.3 and 4.12) to pulses of magnitude 0.2, 0.4, 0.6, 0.8, 1.0, 1.2, and 1.4v. The load line resistance was 25 ohms and the bias current I_0 = 4 ma. The time necessary for the diodes to relax to their stable states was approximately 20 ns. The circuit was slowed down in this case because of the recovery time of the germanium diode (Q5-100) used to shunt the first tunnel diode to obtain a low forward voltage.

4.14 Summary.

1. The speed of operation of the circuit is limited by the duration of the precursor pulse.
2. The switching times of the circuit are dependent on the figures of merit of the individual diodes and on the ratio of the capacitances $C_1 : C_2$; the latter should be in the range $1 \leqslant (C_1 : C_2) < 1.9$ for best response.
3. The duration of the precursor pulse is inversely proportional to δI_V. The temperature dependence of δI_V thus affects the switching time. To reduce the effect of temperature on the switching time, it is advisable to pick diodes having equal valley-current temperature coefficients.
4. A proper choice of series inductance can be made to contribute relatively flat-top output waveforms and to speed up the circuit operation.

5. APPLICATIONS

The multistate composite devices discussed in the preceding chapter can be used to fulfill a variety of digital functions. Some of the possible applications[2] will be discussed briefly, pointing out the advantages and disadvantages of these devices.

5.1 Full Binary Adder.[2],[35]

The circuit is shown in Figure 4-13 and has three inputs driven from voltage sources. The circuit receives "1" or "0" signals on each of its three input channels and yields on its two outputs: Sum and Carry a 0,0; 0,1; 1,0; or 1,1 according to whether none, one, two, or all three input signals are "1". The detailed arithmetic function performed by this circuit is shown in Table 5.1, where X,Y,Z denote the three variable inputs representing the binary numbers to be added, and the Sum and Carry indicate the resultant outputs. There are eight possibilities corresponding to the four output states.

One notes from Table 5.1 that if any of the inputs are biased "ON" (1) or "OFF" (0) a variety of useful logical functions can be performed.[35]

If input Z is so adjusted as to be always "OFF"; the top of Table 5.1 shows that: Sum is assigned "1" if and only if "1" is assigned to either X or Y but not both. The binary exclusive "or" is thus achieved. Furthermore Carry is assigned "1" just

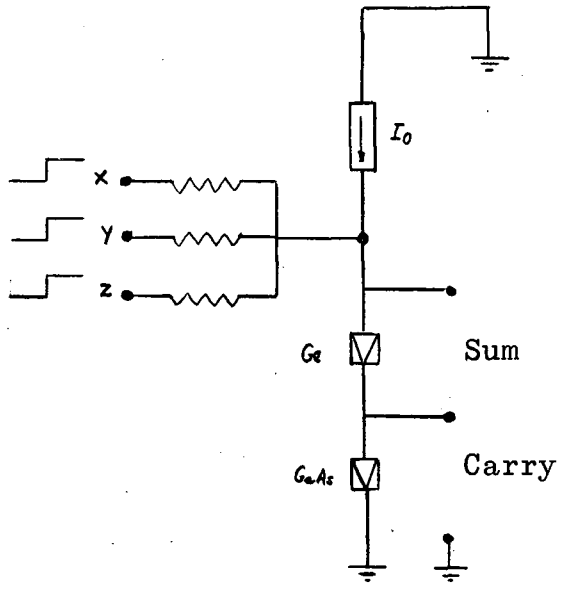

Figure 5-1. Full Binary Adder.

Inputs			SUM	CARRY
X	Y	Z		
0	0	0	0	0
1	0	0	1	0
0	1	0	1	0
1	1	0	0	1
0	0	1	1	0
1	0	1	0	1
0	1	1	0	1
1	1	1	1	1

Table 5.1 Truth table of Full Binary Addition

in that single case where "1" are assigned to both X and Y. The connective "and" is thus realized.

Suppose however that Z is always "ON"; the bottom half of the table reveals that "1" is assigned to Sum just in those cases where both X and Y receive like assignments of "1" or "0". The binary function "if and only if" is achieved. On the other hand, Carry is assigned "0" just in that case where both X and Y are assigned "0"; the "inclusive or" is therefore realized.

There are a number of undesirable features to be noted in the full adder described above. Firstly, the adder has no gain so that amplification at the output is necessary for fan-out. Secondly, the circuit does not provide unidirectionality in the flow of information and isolation from the following stages. This problem is encountered in most tunnel diode circuits and any of the existing methods of cascading[36] can be used. Thirdly, the Sum output is above ground. The adder, however, offers the advantages of circuit simplicity, stability, high speed of operation and compactness which make it well suited for microminiaturization and circuit integration.

5.2 Analog-to-Digital Converter.[37]

The full binary adder described above becomes a two-bit analog-to-digital converter by removing the steady state current I_0 and triggering from a single source. The analog voltage is sampled first, and the sampling pulses are fed to the diode composite circuit. The output of the analog-to-digital converter is available in two forms. The voltage across the tunnel diode

stack is a staircase with incremental steps equal to the forward voltage of the lowest order diode. Binary output is also available by sensing the voltages across the individual diodes. The circuit can be made to encode the analog signal without initial sampling; however, timing problems may arise in this case.

The resolution of the converter can be extended to four bits by using four negative resistance devices (see section 4.3). The extension of the converter's resolution is limited by the presently available diodes.

The following undesirable feature should be noted. An accurate encoder necessitates very carefully controlled v-i characteristics for each diode. This imposes a severe restriction on the generation of a precise predetermined composite characteristic using diodes. Means of obtaining a negative resistance device that avoids this shortcoming have been discussed by Rabinovici and Renton[2]. When the accuracy is not critical, however, the tunnel diode circuit has the advantage of simplicity and high speed of operation. A three-bit encoder was found to have an inherent encoding time of 20 ns.

5.3 Counter.

Counting to a base n can be performed by any device that possesses n distinguishable states which can be attained in a definite sequence. The counter is designed to receive a set of pulses. The system changes state after each incoming pulse, and remains in its new state until the arrival of the next pulse.

The n^{th} incident pulse, in a counter to the base n, is made to trigger a reset circuit which returns the counter to zero, and at the same time delivers a carry output to the next stage.

The multistate tunnel diode circuit can be used as a counter. The diodes are biased from a constant d-c current source I_0 such that $I_{V1} < I_0 < I_{P1}$. Application of pulses of proper amplitude enables the stack to switch from one state to the next. The stack voltage waveform takes the appearance of a staircase. When this staircase reaches the appropriate level, it triggers the reset circuit. Resetting is accomplished by removal of I_0, either by shunting the diodes, or by open-circuiting the source. After the reset pulse, I_0 flows again, and the tunnel diodes are all in their "0" state, ready to form another staircase upon further application of the input pulses.

6. CONCLUSION

The main object of the study is to investigate the behaviour of a simple combination of series-connected tunnel diodes from the static and dynamic points of view. 2^n stable states are obtained by interconnecting n tunnel diodes. While in principle, this technique is valid for any number n, it is at present limited by the semiconductor materials available for the fabrication of tunnel diodes.

In the course of this study, the dynamic behaviour of a single tunnel diode, and the dependence of its switching time on the figure of merit and current overdrive (see Summary, Section 3.5) is discussed to provide a background for the study of the multistate circuit.

A study of the static characteristic of the composite device reveals the necessary conditions for the generation of the required number of stable states. The dynamic behaviour of a two tunnel diode circuit was investigated by digital computer solutions of the non-linear system to obtain an estimate of the switching time. Experimental results compatible with the computer solutions are presented. The most important conclusions drawn from the dynamic investigation are:

(1) The ratio of the capacitances of the two tunnel diodes is an important parameter in determining the operation and speed of the circuit. This ratio must lie within a certain range to ensure the existence of the stable states predicted from the static analysis.

(2) The difference in the diodes' valley currents, and its dependence on temperature affect the switching speed of the composite device.

The multistate circuit has many applications in the performance of digital logic functions such as binary addition, analog-to-digital conversion, and counting. These applications, together with many useful features, make the multistate circuit well worth further investigation. Some of these features are:

1. inherent high speed of operation,
2. simplicity of design,
3. small size and small number of components, which make the circuit well suited for microminiaturization.

APPENDIX I

AI. Measurement of Tunnel Diode Parameters

The tunnel diode equivalent circuit parameters need to be known for nearly every application. For high frequency applications, the junction capacitance and lead inductance are believed to set the upper limit on usable frequency, and to determine the attainable switching speeds. A method of measuring these parameters using a modified General Radio 1602 -A U.H.F. Admittance Bridge is described here.

AI.1 Bias Circuit and Stability

To measure the tunnel diode parameters, some means must be provided to bias the tunnel diode to the desired operating point. If this operating point is in the positive conductance region, then instability does not occur and any convenient biasing arrangement can be used. However, if the desired operating point is in the negative conductance region, then the network may be unstable, and special precautions must be taken to obtain the stability necessary for accurate, steady-state, small-signal measurements. It cannot be overemphasized that the measuring a-c signal across the tunnel diode must be less that 5 mv to prevent errors due to the non-linearity of the diode characteristics.

The 1602-A Admittance Bridge presents a negligible impedance to the unknown, and has a d-c path; therefore, the biasing

configuration shown in Figure AI-1a was used. From the equivalent circuit of Figure AI-1b, with the diode biased in its negative resistance region, the necessary and sufficient conditions for stable operation are:(16)

$$\frac{L}{|r|C} < R_1 + r_d < |r| \qquad \text{...AI-1a}$$

and

$$L < |r|^2 C \qquad \text{...AI-1b}$$

where $|r|$ is the absolute magnitude of the negative resistance at the point under consideration, and L is the total series inductance in the circuit.

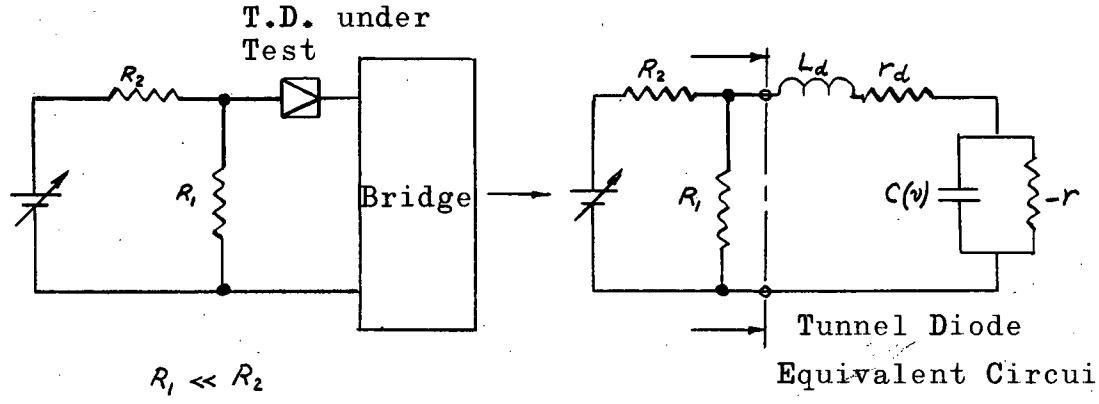

Figure AI-1 (a) Tunnel Diode Test Circuit

(b) Equivalent Circuit

AI.2 Tunnel Diode Test Mount

The test mount for the diode must be designed to minimize stray inductance and capacitance. Figure AI-2 shows a test mount made of readily available General Radio connectors. R_1 is a disc resistor which is essentially non-inductive, has negligible shunt capacitance and is chosen to satisfy the inequalities AI-1 for the diode under test with $L = 2L_d$ (it has been estimated that the bridge and mount inductance is of the same order as L_d). The disc resistor R_1 is located as close to the diode as possible, in order to minimize stray inductance.

AI.3 Experimental Measurements and Results

Figure AI-3a shows the complete diagram of the test circuit and Figure AI-3b shows the bridge external connections.

The series inductance, being constant for a given package design, need be measured only once, using a dummy diode. The series resistance may be measured at conditions of very large reverse voltage.[16]

For the measurement of the diode admittance, the procedure is as follows:

1) The bridge is connected as shown in Figure AI-3b. The connections from the generator and the signal detector have been interchanged. Normally, the signal is applied at the generator end, and it appears without attenuation across the unknown impedance; only a portion of the signal is detected. However, applying the signal from the generator at the detector

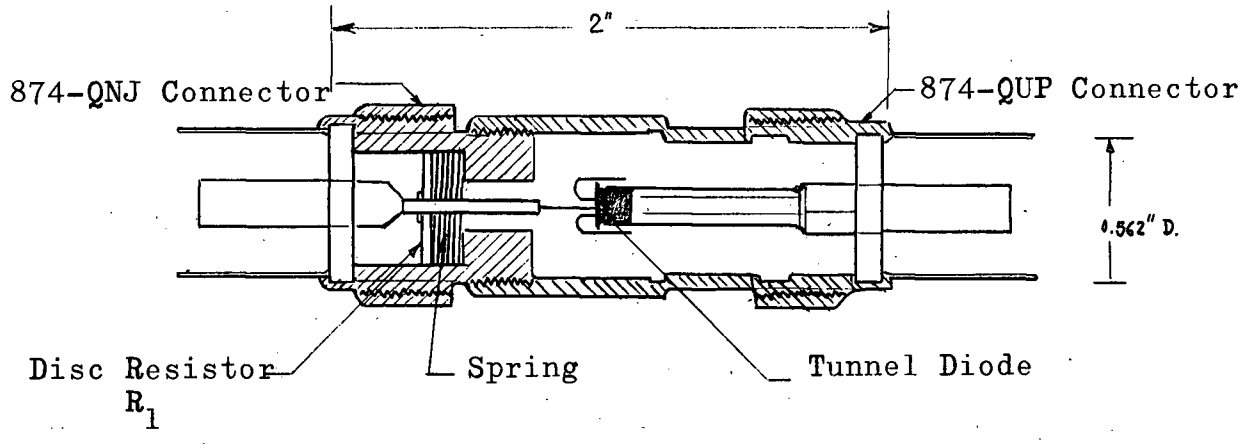

Figure AI-2 Tunnel Diode Coaxial Mount

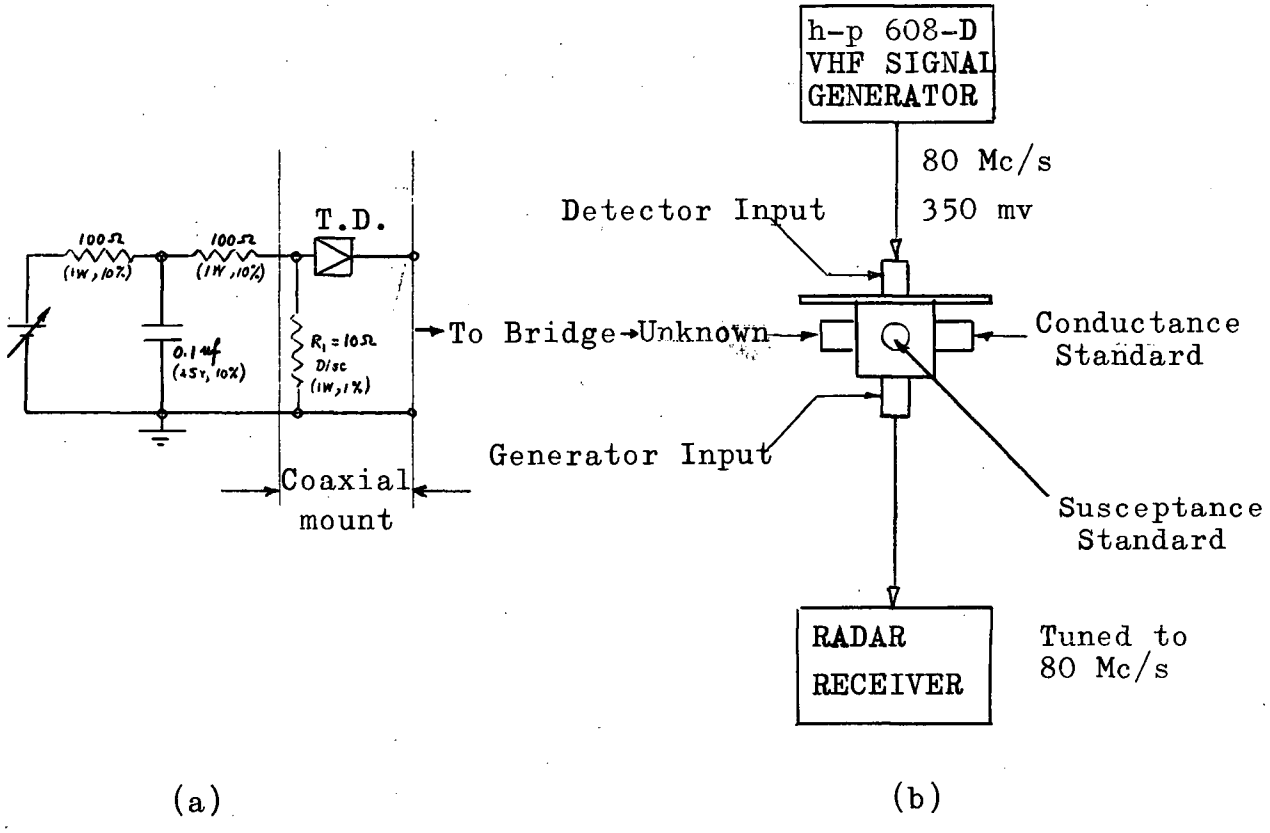

Figure AI-3(a) Diagram of the Test Circuit
(b) Bridge External Connections

terminal ensures that this signal is attenuated (40 db) before being fed to the rest of the bridge circuit: the signal appearing across the tunnel diode can then be of the order of a few millivolts while the detected signal is attenuated by the same amount as for normal operation. Another modification was introduced in the bridge to allow for measurement of negative conductance; this was achieved by rotating the coupling loop associated with the multiplier lever through 90^{o}.

2) The admittance of the diode mount must be measured with the disc resistor, and with a dummy short-circuited diode replacing the actual diode. This admittance value is subtracted from the readings taken with the diode in place to obtain the true diode values for various bias voltages. Figure AI-4 shows the typical admittance characteristics of a Ge 1N2939 diode as a function of bias voltage. Measurements were made at 80 Mc/s. Figure AI-5 shows the experimental variation of capacitance with bias as obtained from the above measurements. The capacitance variation for this specific diode can be expressed as:

$$C(v) = \frac{13.2}{\left[1 - \frac{v}{0.6}\right]^{n}} \text{ pf} \quad n \cong 0.42$$

The total inductance of the mount and diode was found to be 10 nh, from the short-circuited diode reading.

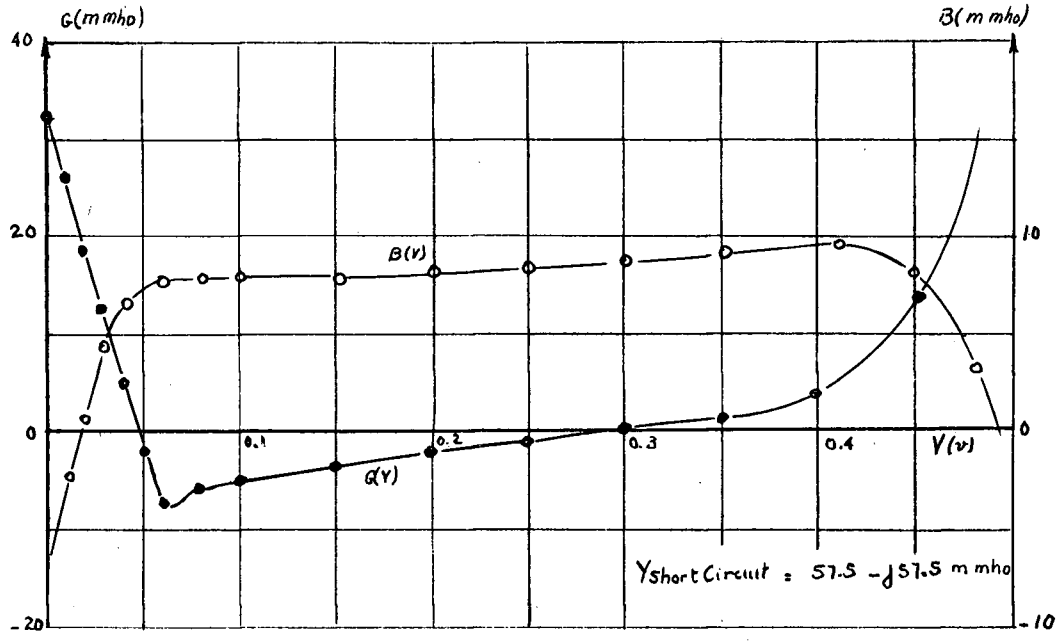

Figure AI-4 Admittance Characteristics of a 1N2939 Diode as a Function of Voltage

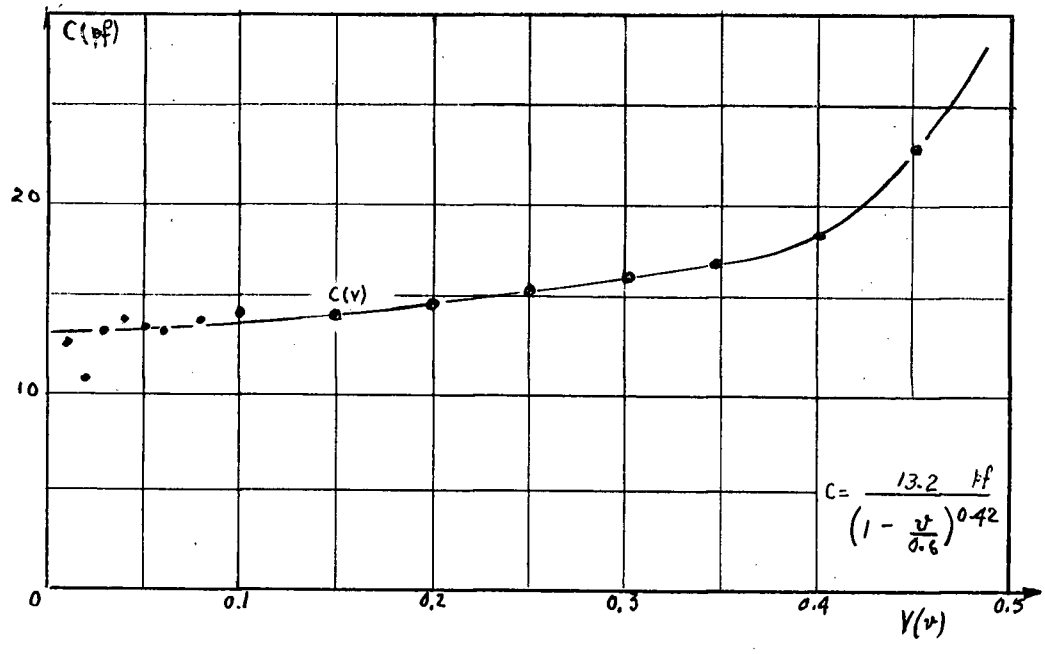

Figure AI-5 Capacitance Variation as a Function of Voltage

APPENDIX II

AII. Methods of Approximating Tunnel Diode Curves

In the study of the tunnel diode switching circuits it is necessary to represent the tunnel diode characteristic $i = f(v)$ in terms of an analytical expression. Most of the theoretical expressions for the tunnel diode characteristic are quite elaborate and unsuccessful in their representation of the observed characteristic . This is mainly due to the fact that the relationship between the various currents flowing through the diode is not yet well understood. The only theoretical expression found to approximate (within 20%) the observed Germanium tunnel diode characteristic is the one developed by Kane.[9],[21] It consists of three components: the theoretical expression for the tunneling current (direct tunneling case), one tenth of the peak current for the excess current, and an expression of the form Kexp (40v) for the diffusion current, where K is a constant. However, this type of representation was found to be quite inadequate for the case of GaAs diodes.

The lack of a satisfactory theoretical expression for the characteristic curve led to the consideration of analytical approximations. Two types of approximations were used: the first is a polynomial approximation, and the second is a two term exponential approximation. Both approximations are concerned with the characteristic in the forward voltage region. In the reverse voltage region, the conduction current can be approximated by an expression of the form $I = \gamma v \exp(-\phi v)$ where γ and ϕ are

constants.

AII.1 Polynomial Approximation

The polynomial approximation was obtained by the method of least mean squares using the IBM 1620 computer. The polynomial contains as many terms as necessary in order to bring the standard error of the dependent variable (current) within the range specified. It should be noted however, that each polynomial generated contains a constant term, and therefore the approximate curve does not go through the origin in the i-v plane. This error is negligible since the portion of the curve near the origin is of little practical importance in most cases. An attempt to make the curve go through the origin resulted in a very poor overall accuracy.

Figure AII-1 shows, for a typical Ge tunnel diode (T1925), the experimental characteristic and the characteristic calculated from a seventh order polynomial. The current difference between the actual and calculated curves is normalized with respect to the peak current and plotted on the lower portion of the graph. It is seen that the approximation is accurate to within $\pm$ 5% over the whole range.

A similar approximation was obtained for a typical GaAs tunnel diode (1N653). In this case a ninth order polynomial ensured a maximum error of $\pm$ 2%, except at the origin, where it is 4.3%. Table AII.1 gives the polynomials for the two diodes.

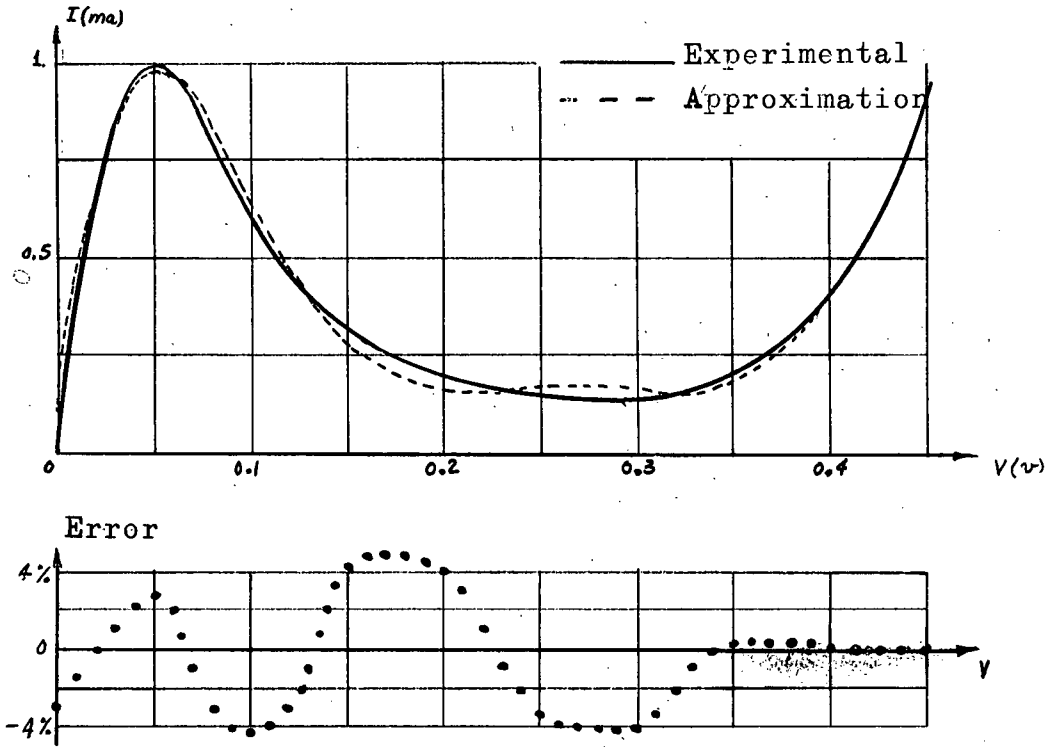

Figure AII-1 T1925 Germanium Tunnel Diode

(a) Actual and Calculated Characteristics
(b) Percent Error Between the Actual and Calculated Characteristics

Diode	Polynomial Approximation (I_p = 1 ma)
Ge	$f(v) = 0.03281 + 44.6474v - 683.013v^2 + 3744.82v^3 - 7211.73v^4 - 5624.81v^5 + 36259.62v^6 - 33114.68v^7$. ...AII-1
GaAs	$f(v) = -0.043518 + 25.372706v - 207.321040v^2 + 676.02962v^3 - 1086.3072v^4 + 899.342610v^5 - 497.832v^6 + 490.08273v^7 - 459.487v^8 + 160.9966v^9$. ...AII-2

Table AII.1 Polynomial Approximations for Tunnel Diodes

AII.2 Two Term Exponential Approximation

The second method of approximation uses a two term exponential expression.[19],[20] The approximation is of the form:

$$f(v) = I_1 + I_2$$

$$= A\,v \exp(-av) + B(\exp(bv) - 1)$$

where a, b, A, B are constants. The first term represents the tunneling current and the second is the diffusion current (see Figure 2-3). The four constants are determined by measuring four sets of current and voltage values at four pilot points to be fitted accurately. Two of the points should be in the tunnel current region and the other points in the diffusion current region. The accuracy of this type of approximation is $\pm$ 10%. Table AII.2 gives the expressions for a Ge (IN2941) and a GaAs (IN 653) diodes. The main advantage of this method of approximation is that it does not require a computer, and different I_P/I_V ratios can be represented for the same type of tunnel diode by changing the two constants B and b. This last feature was found quite useful in the investigation of the series-connected tunnel diode circuit.

It should be noted that Tables AII.1 and AII.2 give the approximations for diodes with peak currents normalized to one ma.

Diode	Exponential Approximation (I_P = 1 ma)
Ge	$f(v) = 0.044v \exp(-16.8v) + 5.4\times10^{-7}(\exp(15.4v)-1)$ ...AII-3
GaAs	$f(v) = 0.026v \exp(-10v) + 1.5\times10^{-7}(\exp(8.76v)-1)$ ...AII-4

Table AII.2 Exponential Approximations for Tunnel Diodes

APPENDIX III

AIII. Factors Influencing the Choice of the Load Line Resistance R in a Multistate Circuit

In choosing a value for R in a two tunnel diode multistate circuit, we must compromise between the necessity of making all the stable states accessible (i.e., R as small as possible), and the requirement that the negative resistance regions be unstable (switching load line; R large). A stability test can be applied to give the minimum load resistance for switching, provided L and $C_k (k=1,2)$ are known.

The problem of determining whether a given point on the static characteristic is stable when the composite device is connected in a given external circuit, can be answered in terms of linear network analysis. The device itself is replaced in the circuit by a small signal linear equivalent circuit, which is valid for small variations of current and voltage about the point in question. The equivalent circuit must include all stray reactive elements. The characteristic equation[32] of the system can be derived from the set of differential equations representing the linearized circuit. If the roots of the characteristic equation have positive real parts, the point investigated is unstable. In other words, the transient following any small displacement from the point is a sum of increasing exponentials.

For the set of two tunnel diodes, the characteristic roots are given as eigenvalues α_0, α_1, α_2 of the matrix:

$$\begin{bmatrix} -\frac{R}{L} & -\frac{1}{\sqrt{C_1 L}} & -\frac{1}{\sqrt{C_2 L}} \\ +\frac{1}{\sqrt{C_1 L}} & -\frac{f_1'^{(*)}}{C_1} & 0 \\ +\frac{1}{\sqrt{C_2 L}} & 0 & -\frac{f_2'^{(*)}}{C_2} \end{bmatrix}$$

evaluated at the point of interest. This matrix is obtained, by adapting, to our specific case, Moser's[33] investigation of the stability of two identical tunnel diodes in series.

With L and C_k fixed, one condition for instability in the negative resistance region is that the load line resistance R should be larger than the magnitude of the larger of the two negative resistances of the diodes. It was found that a value of R = 50 ohms, for the circuit under consideration in section 4.5, gave a fair margin of instability - sufficient for satisfactory switching.

(*) $$f'_k = \frac{d\, f_k(v_k)}{d\, v_k}$$

REFERENCES

1. Esaki, L., "New Phenomenon in Narrow P-N Junctions", Phys. Rev. Letters, Vol. 109, p. 603, 1958.

2. Renton, C., and Rabinovici, B., "Composite Characteristics of Negative Resistance Devices and Their Applications in Digital Circuits", Proc. IRE, Vol. 50, pp. 1648-55, July, 1962.

3. Reed, D.E., "The Variable Capacitance Parametric Amplifier", IRE Trans. PGED, Vol. ED-6, pp. 216-21, April, 1959.

4. Zener, C., "Theory of the Electrical Breakdown of Solid Dielectrics", Proc. Royal Soc., Vol. 145, pp. 523-528, 1934.

5. Kleenknecht, H., "Indium Arsenide Tunnel Diodes", Solid State Electronics, Vol. 2, pp. 133-142, 1961.

6. Esaki, L., and Yajima, T., "Excess Noise in Narrow Germanium P-N Junctions", J. Phys. Soc. Jap., Vol. 13, pp. 1281-1287, November, 1958.

7. Esaki, L., and Miyahara Y., "A New Device Using the Tunneling Process in Narrow P-N Junctions", Solid State Electronics, Vol. 1, pp. 13-21, 1960.

8. Pucel, R.A., "Physical Principles of the Esaki Diode and Some of its Properties", Solid State of Electronics, Vol. 1, pp. 22-33, 1960.

9. Kane, E.O., "Theory of Tunneling", J. Appl. Phys., Vol. 32, pp. 83-91, January, 1961.

10. Lesk, I., Holonyak, N., Davisohn, U., and Aarons, M., "Germanium and Silicon Tunnel Diodes", Wescon IRE Conv. Rec., Vol. 17, pp. 9-31, Part 3, 1959.

11. Chynoweth, A.G., Feldman, W.L., and Logan, R.A., "Excess Current in Silicon Esaki Junctions", Phys. Rev., Vol. 121, pp. 684-94, 1961.

12. Blair, R.R., and Easly, J.W., "Fast Neutron Bombardment of Germanium and Silicon Esaki Diodes", J. Appl. Phys., Vol. 31, pp. 1772-74, October, 1960.

13. Furukawa, Y., "Temperature Dependence of Tunnel Diode Characteristics", J. Phys. Soc. Jap., Vol. 15, p. 1130, June, 1960.

14. Zorzy, P., "Measurement of the Equivalent Circuit Parameters of Tunnel Diodes", General Radio Experimenter, Vol. 35, pp. 3-8, July - August, 1960.

15. Card, H., "Bridge Measurement of Tunnel Diode Parameters", IRE Trans. PGED, Vol. ED8, pp. 215-19, May, 1961.

16. General Electric Co., "Tunnel Diode Manual," First Edition, 1961.

17. Brody, T.P., and Boyer, R.H., "The Evaluation of Esaki Integrals and an Approximation for the Tunnel Diode Characteristics", Solid State Electronics, Vol. 2, pp. 209-15, 1961.

18. Tarnay, K., "Approximation of Tunnel Diode Characteristics", Proc. IRE, Vol. 50, pp. 202-03, February, 1962.

19. Ferendeci, A., "A Study of Tunnel Diode Characteristics", M.S. Thesis, Case Institute of Technology, Cleveland, Ohio, 1961.

20. Ferendeci, A., and Ko, W.H., "A Two Term Analytical Approximation of Tunnel Diode Static Characteristics", Proc. IRE, Vol. 50, pp. 1852-53, August, 1962.

21. Esaki, L., "Characterization of Tunnel Diode Performance in Terms of Device Figure of Merit and Circuit Time Constant", IBM J. of Res. and Dev., Vol. 6, pp. 170-78, April, 1962.

22. Herzog, G.B., "Utilisation de la Diode Tunnel comme Element de Calcul à Vitesse Extremement Elevée", L'Onde Electrique, Vol. 40, pp. 370-381, April, 1961.

23. Sommers, H.S., "Tunnel Diodes as High Frequency Devices", Proc. IRE, Vol. 47, pp. 1201-06, July, 1959.

24. Millman, J., "Vacuum Tube and Semiconductor Electronics", McGraw Hill, New York, p. 121, 1958.

25. Schuller, M., and Gartner, W.M., "Large Signal Circuit Theory for Negative Resistance Diodes in Particular Tunnel Diodes", Proc. IRE, Vol. 49, pp. 1268-78, August, 1961.

26. Gummel, H.K., and Smith F.M., "Margin Considerations for an Esaki Diode OR Gate", Bell Sys. Tech. J., Vol. 40, pp. 230-32, January, 1961.

27. Sarafian, G.P., "Tunnel Diode Threshold Logic", Wescon IRE Conv. Rec., Vol. 9, Part 2, pp. 271-76, 1961.

28. Ralston, A., and Wilf, H.S., Editors, "Mathematical Methods for Digital Computers", Wiley, New York, 1960.

29. Johnston, R.A., and Harbourt, C.O., "Static Characteristics of Combinations of Negative Resistance Devices", Proc. Natl. Electronics Conf., Chicago, Vol. 16, pp. 427-37, 1960.

30. Harbourt, C., "The Dynamic Behaviour of Negative Resistance Devices", Trans. AIEE, Communications and Electronics, pp. 216-22, July, 1962.

31. Herzog, G.B., "Tunnel Diode Balanced Pair Switching Analysis", RCA Rev., Vol. 23, pp. 187-214, June, 1962.

32. Cunningham, W.J., "Introduction to Nonlinear Analysis", McGraw Hill, New York, Ch. 10, 1958.

33. Moser, K.J., "Bistable Systems of Differential Equations with Applications to Tunnel Diode Circuits", IBM J. of Res. and Dev., Vol. 5, PP. 226-40, July, 1961.

34. Rutz, R.F., "Two Collector Transistor for Binary Full Addition", IBM J. of Res. and Dev., Vol. 1, pp. 212-22, July, 1957.

35. Dunham, B., "The Multipurpose Bias Device", IBM J. of Res. and Dev., Vol. 1, pp. 117-129, March, 1957.

36. Sims, R.C., Beck, E.R., and Kamm, V.C., "A Survey of Tunnel-Diode Digital Techniques", Proc. IRE, Vol. 49, pp. 136-148, January, 1961.

37. Beddoes, M.P., and Salama, C.A., "Tunnel Diodes", U.B.C. Engineer, Vol. 2, pp. 18-21, 1962.